Spherical Rotation Dimension Reduction with Geometric Loss Functions

Hengrui Luo¹ and Didong Li^{2,3}

Abstract

Modern datasets witness high-dimensionality and nontrivial geometries of spaces they live in. It would be helpful in data analysis to reduce the dimensionality while retaining the geometric structure of the dataset. Motivated by this observation, we propose a general dimension reduction method by incorporating geometric information. Our Spherical Rotation Component Analysis (SRCA) is a dimension reduction method that uses spheres or ellipsoids, to approximate a low-dimensional manifold. This method not only generalizes the Spherical Component Analysis (SPCA) method in terms of theories and algorithms and presents a comprehensive comparison of our method, as an optimization problem with theoretical guarantee and also as a structural preserving low-rank representation of data. Results relative to state-of-the-art competitors show considerable gains in ability to accurately approximate the subspace with fewer components and better structural preserving. In addition, we have pointed out that this method is a specific incarnation of a grander idea of using a geometrically induced loss function in dimension reduction tasks.

Keywords: dimension reduction, principal component analysis, high-dimensional dataset.

1 Introduction

Modern data analysis presents the challenge of high-dimensionality, where the dataset usually comes as a high dimensional vectors in \mathbb{R}^d , with a very large d. Practitioners usually seek to reduce the dimensionality of the dataset before performing more comprehensive analyses.

¹Lawrence Berkeley National Laboratory, Berkeley, CA, 94720, USA, E-mail: hrluo@lbl.gov
²Department of Computer Science, Princeton University, Princeton, NJ, 08540, USA, E-mail:

didongli@princeton.edu

³Department of Biostatistics, University of California, Los Angeles, Los Angeles, CA 90095, USA.

Dimension reduction (DR) aims at low dimensional representation of high dimension data (Mukhopadhyay et al., 2020; Zhang et al., 2021) to facilitate visualization of the data, subsequent data exploration, and statistical modeling in machine learning (Jolliffe and Cadima, 2016). Along with the difficulty in visualizations and computation, high-dimensional (non-linear) geometries of the space where the dataset lives, would obstruct conventional dimension reduction methods. We would start with datasets that possess nearly spherical shape supports, which we call *spherical datasets*, with examples from directional statistics, among which are text mining (Banerjee et al., 2003, 2005) and medical brain imaging (Dryden et al., 2005). We want to perform DR in order to reduce the dataset but preserve the spherical structures in the support of reduced datasets.

In this paper, we derived a DR method, namely SRCA, that preserves the sphericity of the dataset. This method works for high-dimensional datasets regardless of the retained dimensions and sample sizes. It can also be formulated as an optimization problem that allows generalizations to preserve other geometric structures during reduction.

Before formal expositions, we use toy examples to illustrate these points. The principal component analysis (PCA, Pearson (1901)), probably the most popular linear dimension reduction method, is linear in the sense that the dimension-reduced dataset can be obtained by linear transformations on the original dataset. Linear dimension reduction might destroy not only the geometry but also the topology of the dataset. For example, Figure 1.1 shows two two orthogonal circles parallel to xz and xy hyper-planes respectively in \mathbb{R}^3 . The projection of these two circles to the principal axes given by PCA is shown in Figure 2.1, where only one circular structure is retained in the reduced dataset while the other circular structure is completely destroyed.

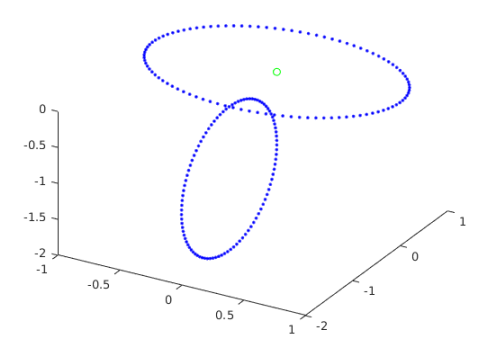


Figure 1.1: A data example where PCA fails, adapted from Luo et al. (2021). Note that the two orthogonal circles only intersect at one point. The DR results are summarized in Figure 2.1

Similar problems in Figure 2.1 arise in various situations with noise as shown in Appendix A. Disruption of these low-dimensional structures in a high-dimensional dataset would diminish the effectiveness of subsequent analysis procedure.

Non-linearity in data facilitated the development of sophisticated non-linear DR methods in the past two decades designed to preserve certain structure in the data, including Multi-Dimensional Scaling (MDS, Kruskal (1978)), Locally Linear Embedding (LLE, Roweis and Saul (2000)), Isomap Tenenbaum et al. (2000), t-distributed Stochastic Neighbor Embedding (tSNE, Van der Maaten and Hinton (2008)), Gaussian Processes Latent Variable Model (GPLVM, Titsias and Lawrence (2010)), Uniform Manifold Approximation and Projection (UMAP, McInnes et al. (2018)), etc.

However, the above mentioned DR methods do not produce an estimate of the non-linear support of the data in the original space, but instead output some low dimensional features in a new space. As a consequence, the performance of the DR method, usually presented by the mean squared distance between observations and their projections to the estimated space, is not well-defined. The mean squared distance is not only a straightforward metric that can be used to define a DR method, but allows cross-validation for tuning parameters in DR methods. For example, in PCA, the mean squared distance, also known as the geometric loss, is used to determine the number of principal components and hence the dimension of the low dimensional linear subspace. As a result, DR methods that provides a low dimensional, potentially non-linear, estimate benefit the follow-up analysis.

A recent attempt to develop a non-linear DR algorithm that estimating the underlying manifold in the originals pace is Li et al. (2022), which focused on spherical version of PCA (SPCA) and proposed a novel two-step method which allows us to conduct dimension reduction and learn the shape of spherically distributed datasets. SPCA works well for dataset living on a low-dimensional sphere $S \cong \mathbb{S}^{d'} \subset \mathbb{R}^d$ where the sphere dimension $d' \leq d-1$. Intuitively, this problem is well-defined as an estimation problem of the (center, radius and dimension of) sphere S. The geometric constraints imposed by the SPCA method helps us to identify low-dimensional structures in the reduced dataset, which turns out to be exceedingly challenging (Luo et al., 2020). The objective of SPCA is not to minimize the geometric loss defined by the mean square distance. Instead, an algebraic loss based algorithm is adopted for a closed-form solution of SPCA.

However, both PCA and SPCA fails when the sample size n < d', the retained dimension (i.e., the dimension of the reduced dataset, the formal definition would be introduced below) and are not easily applicable to high dimensional datasets. For instance, in the gene expression data, d is the number of genes, that is often over 20,000

and the retained dimension d' is often chosen to be a couple of hundreds with the largest variability. While the sample size could be much smaller, for example, less than 20 for certain tissues in the Genotype-Tissue Expression (GTEx) dataset (Consortium, 2020). In fact, most existing dimension aforementioned reduction methods can not handle n < d'. Our proposed method can handle arbitrary d' regardless n and d.

In the current paper, we explore a geometrically induced loss function with a fully statistically principled dimension reduction approach called Spherical Rotation Component Analysis (SRCA), which generalizes SPCA in that all estimators are estimated in one single step together with a sparse version designed for high-dimensional data. Our method also exemplifies a grander belief that any dimension reduction should be guided by the need of its subsequent analyses and respect the structure in the original dataset.

The organization of the rest of paper is as follows. In the Section 2, we first revisit the PCA and SPCA in Section 2.1. This discussion motivates our design of a geometric loss function in Section 2.2, based on which we formulate optimization problems that minimizes this specific loss functions. Then, we proposed our dimension reduction algorithm in Section 2.3 and wrap the section up with a sparse penalized version of the procedure in Section 2.4. We turn to theoretical guarantees in Section 3. Algorithmic convergence for the optimization problem and its l_1 variant via gradient descent is discussed in Section 3.1. Then the MSE minimizing property would be elicited from our design of geometric loss in Section 3.2. Consistency and asymptotics are discussed in Section 3.3. Practical examples and numerical experiments are detailed in Section 4. We first investigate structure preserving property of our method against state-of-art methods qualitatively in Section 4.2. Then we provide quantitative measurements for DR methods using coranking matrix in Section 4.3. Based on these findings, we briefly discuss parameter selection in Section 4.4 and wrap the section up with observations in Section 4.5. The paper concludes with our findings in Section 5, with directions of possible future work.

2 Methodology

In this section, we describe the proposed procedure that aims at minimizing a geometric loss function, hence the mean squared errors between the original data points x_i and dimension-reduced data points $\hat{x_i}$.

Retained dimension. In the following discussions, we denote the intrinsic dimension of the support of reduced dataset by d' and call it the *retained dimension* or reduced

dimension. Note that the convention of taking embedded dimension as the reduced dimension is adopted from time to time. For instance, if the reduced dataset lies in \mathbb{S}^1 embedded into \mathbb{R}^2 , then we would consider the dimensionality of the reduced data to be d'=1 not 2 because that \mathbb{S}^1 is a manifold of intrinsic dimension 1.

2.1 PCA and SPCA Revisited

To begin with, we recall that PCA finds a low-rank linear subspace from observations $\mathcal{X} = \{x_1, \dots, x_n\} \subset \mathbb{R}^d$, by minimizing the sum of squared error loss function (Pearson, 1901):

$$\min_{V \in \mathbb{R}^{d \times d'}} \sum_{i=1}^{n} \|x_i - \widehat{x_i}\|^2 = \sum_{i=1}^{n} \|x_i - \bar{x} - VV^T(x_i - \bar{x})\|^2, \text{s.t. } V^TV = I_{d'}.$$

where $\bar{x} = \frac{1}{n} \sum_{i=1}^{n} x_i$ is the sample mean calculated in \mathbb{R}^d . The solution of this optimization problem finds a rotation matrix V that determines a hyper-plane, therefore, we also call the hyper-plane a solution to PCA.

In an optimization perspective, alternatively, we treat the PCA as an optimization problem for a given (geometric) loss function (Journée et al., 2010), which describes the l_2 errors between the observation and the hyperplane. The advantage of this approach of treating PCA as an optimization problem is that it provides flexibility, algorithms and fits better in the manifold learning context (Erichson et al., 2020; Journée et al., 2010).

In a probabilistic perspective, the PCA can be viewed as constructing a low-rank approximation to the original likelihood (in a total least square setting). Subsequent researches concern on generalization from the probabilistic perspective is to use kernel transformations for non-linear subspace (Schölkopf et al., 1997, 1998). The advantage of this approach of regarding PCA as a low-rank likelihood approximation problem is that both statistical inference and the large sample behavior can be formalized.

SPCA (Li et al., 2022) aims to find the best sphere S. Different from the solution hyperplane of PCA, the solution of SPCA is a sphere with center c and radius r lying in linear subsapce V to fit the data. SPCA is not minimizing the sum of squared distance between observation and the sphere, also known as the geometric loss. In certain applications like manifold learning, minimizing the geometric loss is of great interests, which requires a one-step algorithm. The desired one-step algorithm is not studied in the original paper (Li et al., 2022) since the problem is theoretically more complicated and does not admit a closed-form solution (See Appendix F). In this paper, we develop a geometric loss based one-step non-linear DR method that works for all d'.

2.2 Geometric Loss Function

Given a sphere centered at c with radius r, we first assume that it lies in a hyper-plane parallel to a coordinate hyper-plane in \mathbb{R}^d determined by $\mathcal{I} \subset \{1, \dots, d\}$. We denote such low-dimensional "sub-sphere" by $S_{\mathcal{I}}(c,r)$ and use the notation $I_{\mathcal{I}}$ to denote an identity matrix with ones in (i,i)-th entries, $i \in \mathcal{I}$ but zeros in the rest entries, then the point-to-sphere distance from a generic point x_i to this sphere can be expressed as

$$d(x_i, S_{\mathcal{I}}(c, r))^2 = (x_i - c)^T I_{\mathcal{I}^c}(x_i - c) + \left(\sqrt{(x_i - c)^T I_{\mathcal{I}}(x_i - c)} - r\right)^2$$
$$= ||x_i - c||^2 + r^2 - 2r\sqrt{(x_i - c)^T I_{\mathcal{I}}(x_i - c)}.$$

If the sphere lies in a coordinate hyper-plane after a linear transformation determined by matrix W, we can generalize this loss into

$$d(x_i, S_{\mathcal{I}}(c, r))^2 = (x_i - c)^T W I_{\mathcal{I}^c}(x_i - c) + \left(\sqrt{(x_i - c)^T \sqrt{W}^T I_{\mathcal{I}} \sqrt{W}(x_i - c)} - r\right)^2$$
$$= (x_i - c^T) W(x_i - c) + r^2 - 2r \sqrt{(x_i - c)^T \sqrt{W}^T I_{\mathcal{I}} \sqrt{W}(x_i - c)}.$$

Note that the assumption that the sphere lies in a coordinate plane is essential, otherwise no closed form expression can be written. With this point-to-sphere distance, the (geometric loss) function can be written as

$$\mathscr{L}(c, r, \mathcal{I} \mid \mathcal{X}) = \sum_{i=1}^{n} \left(\|x_i - c\|^2 + r^2 - 2r\sqrt{(x_i - c)^T I_{\mathcal{I}}(x_i - c)} \right).$$

With consideration of transformation matrix W, we have a more general form:

$$\mathscr{L}(c,r,\mathcal{I}\mid\mathcal{X},W) = \sum_{i=1}^{n} \left((x_i - c)^T W(x_i - c) + r^2 - 2r \sqrt{(x_i - c)^T \sqrt{W}^T I_{\mathcal{I}} \sqrt{W}(x_i - c)} \right).$$

Then our dimension reduction procedure can be described as solving the optimization problem below:

$$\min_{\mathcal{I} \subset \{1, \cdots, d\}, c \in \mathbb{R}^d, r \in \mathbb{R}^+} \mathcal{L}(c, r, \mathcal{I} \mid \mathcal{X}, W)$$
(2.1)

$$= \min_{\mathcal{I} \subset \{1, \dots, d\}, c \in \mathbb{R}^d, r \in \mathbb{R}^+} \sum_{i=1}^n \left((x_i - c)^T W(x_i - c) + r^2 -2r \sqrt{(x_i - c)^T} \sqrt{W}^T I_{\mathcal{I}} \sqrt{W} (x_i - c) \right), \text{ s.t.} |\mathcal{I}| = d' + 1$$
 (2.2)

Using the loss function defined in (2.1), we can estimate the center c, radius r and \mathcal{I} simultaneously by solving the optimization problem.

On one hand, since there are at most 2^d possible choices of \mathcal{I} , it is straightforward to verify that this one-step optimization problem (2.1) can be equivalently solved in a two-step procedure: Pick one subset of indices $\mathcal{I} \subset \{1, \dots, d\}$ first and then estimate the center c and radius r of the dataset \mathcal{X} .

On the other hand, this optimization problem can also be solved iteratively on variables \mathcal{I}, r, c , the binary search can be the first step, after pinning down the index set \mathcal{I} , we can estimate center c and radius r:

- 1. Given c and r, we perform an exhaustive binary search among all possible \mathcal{I} .
- 2. Given \mathcal{I} and c, we can take derivative of $\frac{\partial \mathcal{L}}{\partial r} = 0$ and yield:

$$r = \frac{1}{n} \sum_{i=1}^{n} \sqrt{(x_i - c)^T \sqrt{W}^T I_{\mathcal{I}} \sqrt{W} (x_i - c)}.$$

3. Given \mathcal{I} and r, we can take derivative of $\frac{\partial \mathcal{L}}{\partial c} = 0$ and yield:

$$\frac{\partial \mathcal{L}}{\partial c} = \sum_{i=1}^{n} \left(-2W(x_i - c) + 2r \frac{I_{\mathcal{I}}\sqrt{W}(x_i - c)}{\sqrt{(x_i - c)^T\sqrt{W}^T}I_{\mathcal{I}}\sqrt{W}(x_i - c)}} \right) = 0.$$

Observe that if $j \in \mathcal{I}$, then the j-th coordinate of the second term is zero, so we have $c_j = \frac{1}{n} \sum_{i=1}^n x_{i,j}$ for any $j \in \mathcal{I}^c$. For $j \in \mathcal{I}$, it's hard to find analytic solution but gradient descent could yield us a numerical solution.

So far, we always assume that the underlying support $S_{\mathcal{I}}$ has coordinate axes that are parallel to the coordinate axes. To make this assumption more realistic, we propose to rotate the dataset \mathcal{X} so that it can be viewed in a position that its axes are parallel to the coordinate axes, therefore, the above derivations of geometric loss function based on point-to-sphere distance applies to the rotated dataset. After rotating the ellipsoid so that the axes are parallel to the coordinate axes, we solve the optimization problem (2.1) for the rotated dataset and rotate it back to obtain reduced dataset. The full algorithm is described in Section 2.3 and elaborated in Appendix C.

The exhaustive binary search over 2^d possible subsets is computationally expensive. We observe that the essence of the above optimization problem is a subset selection of index set $\{1, \dots, d\}$. We can rephrase the optimization problem (2.1) in the following

way:

$$\min_{c \in \mathbb{R}^d, r \in \mathbb{R}^+} \sum_{i=1}^n \left((x_i - c)^T W(x_i - c) + r^2 - 2r \sqrt{(x_i - c)^T \sqrt{W}^T v^T I v \sqrt{W} (x_i - c)} \right) \quad \text{s.t. } ||v||_{l_0} = d' + 1, \quad (2.3)$$

Since l_0 -norm is not convex, the solution of this problem requires a brute-force step in finding optimal v whose entries are either 0 or 1 (and hence \mathcal{I} since $v^T I v = I_{\mathcal{I}}$), as detailed in Algorithm 2.

However, this does not solve the computational difficulty of the above optimization problem. Instead of using l_0 directly as in the original problem, we can consider following computationally less expensive alternative:

$$\min_{c \in \mathbb{R}^d, r \in \mathbb{R}^+} \sum_{i=1}^n \left((x_i - c)^T W(x_i - c) + r^2 - 2r \sqrt{(x_i - c)^T \sqrt{W}^T v^T I v \sqrt{W} (x_i - c)} \right) \quad \text{s.t. } \|v\|_{l_k} \le d' + 1, \quad (2.4)$$

where $k \geq 1$, equivalently, we consider the l_k norm instead of l_0 norm (usually l_1 is sufficient). Usually we would use $||v||_{l_1} = d' + 1$ as the relaxation, but other convex norms could be of use as well. This kind of relaxation is proposed in optimization (Boyd et al., 2004). As a practical suggestion, when there are more than 500 combinations of binary indices to be searched exhaustively, we would recommend ℓ_1 relaxation as in (2.4).

In the rest of the paper, we would study the case W = I unless other wise is stated. For very high-dimensional dataset, the empirical performances for l_0 and l_1 penalties are similar, we also add one more estimation step for c, r in order to obtain better results, details can be found in Algorithm 2.

2.3 SRCA Method

We call the method we discussed above and formulate below the *spherical rotation dimension reduction (SRCA) method with geometric loss functions* designed for spherical dataset. The rotation can be chosen according to the types of datasets as appropriate in the procedure as will be discussed in Sec.4.4. In addition to spherical datasets, our method has been shown to respect the topologically non-trivial datasets as well (See Appendix B). The best sphere found by SRCA is called the solution of SRCA.

The key steps of our proposed SRCA dimension reduction method can be simply

summarized into a "Rotate-Optimize-Project" scheme as follows, with algorithms detailed in Appendix C:

- (Rotate: Conduct the rotation.) With the chosen rotation method, we construct a rotation matrix R based on the datset \mathcal{X} . We translate and rotate the dataset \mathcal{X} to standard position $(\mathcal{X} \bar{\mathcal{X}})R$, so that we can realistically assume that the axes of the ellipsoid are parallel to the coordinate axes (Jolliffe, 1995). Hererafer, we assume that the dataset has been rotated and use the same notation \mathcal{X} so $R = I_d$.
- (Optimize: Solve the optimization for the best d' + 1 axes.) We perform dimension reduction based on the geometric loss function discussed above. As we stated in (2.3) above, we conduct dimension reduction by minimizing the loss function based on the point-to-sphere distance to the estimated sphere $S_{\mathcal{I}}$, hence obtain the optimal v_{opt} and the optimal index set \mathcal{I}_{opt} .

$$(v_{\text{opt}}, c_{\text{opt}}, r_{\text{opt}}) = \arg\min_{c \in \mathbb{R}^d, r \in \mathbb{R}^+} \sum_{i=1}^n \left((x_i - c)^T W(x_i - c) + r^2 - 2r \sqrt{(x_i - c)^T \sqrt{W}^T v^T I v \sqrt{W} (x_i - c)} \right) \text{ s.t. } \|v\|_{l_0} = d' + 1,$$

$$(2.5)$$

where the constraint can be relaxed by $||v||_{l_k} \le d' + 1$.

• (Project: project onto the optimal sphere.) Now we project the datapoints back into full space with the chosen dimension and axes, putting x_i back onto the sphere $S(c_{\text{opt}}, r_{\text{opt}})$ with estimated center c_{opt} and radius r_{opt} , getting the SRCA projection:

$$\widehat{x}_i = c_{\text{opt}} \cdot v_{\text{opt}} + r_{\text{opt}} \frac{(x_i - c_{\text{opt}}) v_{\text{opt}}^T I v_{\text{opt}}}{\|(x_i - c_{\text{opt}}) v_{\text{opt}}^T I v_{\text{opt}}\|}.$$
(2.6)

Then we show that SRCA is a generalization to SPCA. Suppose that the \mathcal{X} has already been standardized to be mean zero and rotated by PCA rotation matrix. Let $(c_{\text{SPCA}}, r_{\text{SPCA}}, V_{\text{SPCA}})$ be the solution of SPCA, then the columns of V_{SPCA} are $v_j = e_j$ for $1 \leq j \leq d' + 1$, where e_j is the standard basis of \mathbb{R}^d . So rank(V) = d' + 1 and V represents a (d' + 1)-dimensional linear subspace of \mathbb{R}^d . The SPCA projection is

$$\widehat{x}_i = c_{\text{SPCA}} + r_{\text{SPCA}} \frac{(x_i - c_{\text{SPCA}}) V_{\text{SPCA}} V_{\text{SPCA}}^T}{\|(x_i - c_{\text{SPCA}}) V_{\text{SPCA}} V_{\text{SPCA}}^T\|}.$$
(2.7)

Observe that Equation 2.7 coincides with Equation 2.6 when $v_{\text{opt}} = (1, \dots, d' + 1) \in \mathbb{R}^{d'+1}$ and the rotation in step 1 is the PCA rotation. That is, SPCA always find

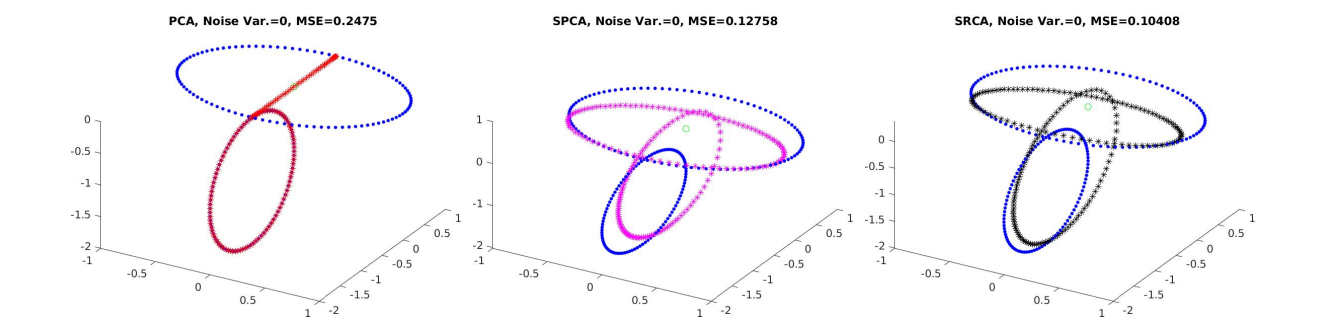


Figure 2.1: The dimension-reduced dataset from the example shown in Figure 1.1. The green dot represents the origin (0,0,0). The original dataset are blue points. On the left panel, the PCA dimension-reduced dataset are red stars. On the middle and right panels the dimension-reduced dataset processed by SPCA and SRCA, in magenta and black stars. SRCA has the smallest MSE.

the d' + 1 dimensional linear subspace spanned by the first d' + 1 eigenvectors of the covariance matrix so is a special case of SRCA.

We briefly showed in Figure 2.1 the difference between PCA and SRCA method using the example we discussed in Figure 1.1 with more examples with realistic noises in Appendix A. It is not hard to see that SPCA and SRCA method respects the topology of the original dataset much better under the same d'. PCA does not retain the circular structure but SRCA puts both circles onto a larger 1-sphere congruent to \mathbb{S}^1 . We would provide quantitative comparative evidence later.

2.4 Sparse Penalty

High dimension data are often assumed to be sparse, while SPCA fails to incorporate sparsity. In this section, we provide a new version of SRCA with sparse penalty, which only involves an additional penalty term in the loss function we designed.

Recall that the objective loss function with a weighted matrix W in our method is

$$d(x_i, S_{\mathcal{I}}(c, r))^2 = (x_i - c)^T W(x_i - c) + r^2 - 2r \sqrt{(x_i - c)^T \sqrt{W}^T I_{\mathcal{I}} \sqrt{W} (x_i - c)}$$

which involves only the point-to-sphere distance from x_i to the estimated sphere surface $S_{\mathcal{I}}$ (based on dataset $\mathcal{X} = \{x_1, x_2, \dots, x_n\}$). One problem we wish to address when there exists sparsity in the dataset in the procedure of dimension reduction, is that we want the sparsity being preserved.

To be more precise, if x_i 's have most coordinates zeros except for a few, then we want

the reduced dataset \hat{x}_i to have a similar property. This can be achieved by penalizing $||I_{\mathcal{I}}(x_i - c)||_1$ in the optimization problem, which encourages the estimated sphere so that the data are in the affine subspace centered at c while parallel to the coordinate planes. This is different from the l_1 relaxation we propose above. The l_1 relaxation we proposed above is an approximation to the constraints we imposed on the binary optimization problem. Here, we directly penalize the reduced coordinates. Note that after the optimal rotation, sparsity would not be disturbed. The optimization problem we need to solve is as follows:

$$\min_{c \in \mathbb{R}^d, r \in \mathbb{R}^+} \sum_{i=1}^n \left((x_i - c)^T W(x_i - c) + r^2 - 2r \sqrt{(x_i - c)^T \sqrt{W}^T v^T I v \sqrt{W} (x_i - c)} \right) + \lambda \|I_{\mathcal{I}}(x_i - c)\|_1, \tag{2.8}$$
s.t. $\|v\|_{l_k} \le d' + 1, \lambda > 0,$

with a tuning parameter $\lambda > 0$. $||v||_{l_k} \leq d' + 1$ can be $||v||_{l_k} = d' + 1$ Now we can see that the penalty we impose would be part of the the objective function instead of constraints. This feature of l_1 constraint allows us to perform dimension reduction in a high-dimensional input space with SRCA.

3 Theoretical Results

We have established the procedure for our propose method SRCA in an algorithmic way. Next, we discuss and provide some theoretical results that guarantee performance of the SRCA in applications. Essential proofs and calculations are deferred to appendices.

3.1 Algorithmic Convergence

Unlike the SPCA, the SRCA does not have a closed form solution (i.e., analytic expression of center and radius estimates in terms of dataset \mathcal{X}) but relies on the solution to an optimization problem. Therefore, the convergence of this optimization becomes central in our theory development. For the theoretic discussions in this section, we consider the most general form of loss function with a general W for clarity.

We briefly discuss the convergence guarantee for the algorithm we designed. In the binary search situation, for each fixed choice of indices, we compute the gradient of loss function. With mild assumptions, the gradient descent would provide linear convergence. In the l_1 relaxation situation, the problem can be formulated as a Lagrange multiplier with inequality constraints.

If the optimization problem (2.5) has solutions, then the solution is clearly unique. This is because there are only finitely many v such that $||v||_{l_0} = d' + 1$, the standard algorithm would exhaustively search all possible values of v.

To this ends we provide a basic convergence for a sub-problem in our Algorithm 1 via the gradient descent algorithm of positive constant step size. The sub-problem is defined by the following loss function:

$$\mathcal{L}_v(c, r | \mathcal{X}, W) = \mathcal{L}_v(c, r) := \sum_{i=1}^n \left((x_i - c)^T W (x_i - c) + r^2 \right)$$
(3.1)

$$-2r\sqrt{(x_i-c)^T\sqrt{W}^Tv^TIv\sqrt{W}(x_i-c)}$$
(3.2)

The following theorem guarantees the convergence of SRCA.

Theorem 1. For a fixed vector v (or equivalently $I_{\mathcal{I}}$), if we assume that $||x_i - c|| \le R_1$, $\forall i = 1 \cdots, n, \ r \le R_2$ and $|\lambda_{\max}(W)| \le R_3$, where $\lambda_{\max}(\cdot)$ denotes the largest eigenvalue, then for a positive finite constant step size independent of the iteration number k, the gradient descent algorithm (c.f., the setting in Boyd et al. (2004, 2003)) converges to the optimal value in the following sense,

$$\lim_{k\to\infty} \mathscr{L}_{v,k} \to \mathscr{L}_v^*$$

where $\mathcal{L}_{v,k} = \mathcal{L}_v(c_k, r_k)$, (c_k, r_k) is the value in the k-th iterative step in the gradient descent algorithm, \mathcal{L}_v^* denotes the minimum of the loss function for this fixed v.

Proof. See Appendix
$$G.1$$

These results justify that for a fixed v (or equivalently \mathcal{I}) we can solve the subproblem defined by the above function, and since we conduct an exhaustive search for the vector v, we can find the solution to the original problem (2.5) as well.

A direct corollary is that if the data x_1, \dots, x_n are exactly from a sphere, then SRCA will recover this sphere:

Corollary 1. Assume $x_i \in S_{\mathcal{I}_0}(c_0, r_0)$, $\forall i = 1, \dots, n \text{ and } n > d' + 1$. Let $\widehat{\mathcal{I}}_k, \widehat{c}_k, \widehat{r}_k$ be the solution of SRCA after k iteration, then

$$(\widehat{\mathcal{I}}_k, \widehat{c}_k, \widehat{r}_k) \xrightarrow{k \to \infty} (\mathcal{I}_0, c_0, r_0).$$

Proof. It is clear that $\mathscr{L}(c_0, r_0, \mathcal{I}_0) = 0$ and $\widehat{\mathcal{I}}_k, \widehat{c}_k, \widehat{r}_k \to \arg\min \mathscr{L}$ by Theorem 1, it suffices to show $(c_0, r_0, \mathcal{I}_0)$ is the unique zero of L. Recall that $\mathscr{L}(c, r, \mathcal{I}) = 0$ if and only

if all all x_i 's are exactly on sphere $S(c, r, \mathcal{I})$, and that d' + 2 points uniquely determine a d' dimensional sphere, then the uniqueness follows from the assumption n > d' + 1. \square

3.2 Mean Square Error (MSE) Comparison

In this section, we consider the theoretic behavior of SRCA when the underlying dataset is assumed to be already observed and fixed. The following theorem compares the MSE of PCA, SRCA (when the rotation is chosen by PCA) and SPCA:

Theorem 2. Given data x_1, \dots, x_n in a bounded subset of \mathbb{R}^d , let H be the best hyperplane obtained by PCA, S_1 be the sphere obtained by SPCA and S_2 be the sphere obtained by SRCA with rotation provided by PCA, then

$$\sum_{i=1}^{n} d^{2}(x_{i}, S_{2}) \leq \min \left\{ \sum_{i=1}^{n} d^{2}(x_{i}, H), \sum_{i=1}^{n} d^{2}(x_{i}, S_{1}) \right\}.$$

Proof. First we compare SRCA with PCA. Assume $||x_i|| \leq \alpha$ for any i, then for any $\epsilon > 0$, there exists a sphere S_{ϵ} such that $d(y, S_{\epsilon}) \leq \epsilon$ for any $y \in H$ with $||y|| \leq \alpha$ (Li et al., 2022). Intuitively, a hyperplane can be approximated by a sphere with infinite radius. Let $\hat{x}_i = \arg\min_{y \in H} d(x_i, y)$ be the linear projection of x_i to hyperplane H, then by the triangle inequality,

$$d(x_i, S_{\epsilon}) \le d(x_i, \widehat{x}_i) + d(\widehat{x}_i, S_{\epsilon}).$$

Since the linear projection of a bounded set is still bounded, $d(\hat{x}_i, S_{\epsilon}) \leq \epsilon$. By the definition of SRCA,

$$\sum_{i=1}^{n} d^{2}(x_{i}, S_{2}) \leq \sum_{i=1}^{n} d^{2}(x_{i}, S_{\epsilon}) \leq \sum_{i=1}^{n} d^{2}(x_{i}, H) + 2\epsilon \sum_{i=1}^{n} d(x_{i}, H) + n\epsilon^{2}.$$

Let $\epsilon \to 0$, we conclude that

$$\sum_{i=1}^{n} d^2(x_i, S_2) \le \sum_{i=1}^{n} d^2(x_i, H).$$

Then we compare SRCA with SPCA. Since the objective function \mathcal{L} , which defines SRCA, is $\min_{S} \sum_{i=1}^{n} d^2(x_i, S)$, it follows from $S_1 \subset H$ that

$$\sum_{i=1}^{n} d^2(x_i, S_2) \le \sum_{i=1}^{n} d^2(x_i, S_1).$$

3.3 Asymptotics of SRCA

In this section, we consider the asymptotic behavior of SRCA when the underlying dataset is assumed to be drawn from a probabilistic distribution.

To yield the asymptotic results, we need to take the perspective of robust statistics as mentioned in the end of Section 2.4. The asymptotic theory here is a specific case of empirical risk minimization. With a mild technical assumption that the parameter $\theta = (c, r) \in \Theta := [-C, C]^d \times [R_0, R] \subset \mathbb{R}^d \times \mathbb{R}^+$ for some $C, R_0, R \in (0, \infty)$, our loss function and optimization problem can be expressed as

$$\min_{\mathcal{I}\subset\{1,\cdots,d\},c\in[-C,C]^d\subset\mathbb{R}^d,r\in[R_0,R]\subset\mathbb{R}^+}\mathcal{L}(c,r,\mathcal{I}\mid\mathcal{X},W)$$
(3.3)

$$= \min_{\mathcal{I} \subset \{1, \dots, d\}, c \in [-C, C]^d \subset \mathbb{R}^d, r \in [R_0, R] \subset \mathbb{R}^+} \sum_{i=1}^n \left((x_i - c)^T W(x_i - c) + r^2 - \frac{1}{2} \left((x_i - c)^T \sqrt{W(x_i - c)} + r^2 - \frac{1}{2} \sqrt{W(x_i - c)} \right) \right) \text{s.t.} |\mathcal{I}| = d' + 1$$
(3.4)

For a fixed \mathcal{I} , it can be written into the minimum problem in the form of (3.1) in Huber (2004), i.e.,

$$\rho(x;\theta) = \left((x_i - c)^T W(x_i - c) + r^2 - 2r \sqrt{(x - c)^T \sqrt{W}^T I_{\mathcal{I}} \sqrt{W} (x - c)} \right)$$

Correspondingly, we can write Huber's ψ -type function of ρ as $\psi(\theta) = \frac{\partial \rho(\theta)}{\partial \theta}$.

Classical style asymptotic results are as below and their proofs are routinely presented in Appendix G. Theorem 3 states that with mild assumptions, the estimates T_n obtained by solving SRCA would estimate the center and radius of the spherical space consistently, corresponding to Huber's ρ -type estimator consistency (Huber et al., 1967); Theorem 4 states that with more stringent conditions on continuity of T_n , asymptotic normality of these estimators can also be formulated into Huber's ψ -type normality. Note that to apply these two asymptotic results, we have to make mild assumptions on the parameter space and also assumed that we already know the retained dimension d' + 1. In practice, these are not very restrictive assumptions.

Theorem 3. Suppose that the index vector \mathcal{I} is fixed and the parameter $\theta = (c, r) \in \Theta := [-C, C]^d \times [R_0, R] \subset \mathbb{R}^d \times \mathbb{R}^+$ for some $C, R_0, R \in [0, \infty)$ and the samples $x_1, \dots, x_n \in \mathbb{X} = \mathbb{R}^d$ of size n are i.i.d. drawn from the common distribution P. P has finite second moments on the probability space $(\mathbb{X}, \mathcal{A}, \nu)$ with Borel algebra \mathcal{A}

and Lebesgue measure ν . Then the consistent estimator T_n for parameter $\theta = (c, r)$ defined by

$$\frac{1}{n} \sum_{i=1}^{n} \rho(x_i; T_n) - \inf_{\theta \in \Theta} \frac{1}{n} \sum_{i=1}^{n} \rho(x_i; \theta) \xrightarrow{n \to \infty} 0, a.s. P$$

would converge in probability and almost surely to θ_0 w.r.t. P (for the parameter values θ_0 defined on page 50). Particularly, T_n can be realized as a solution to our optimization problem (3.3) above.

Proof. See Appendix
$$G.2$$
.

Unlike the Theorem 1 which concerns the convergence of algorithm, we assume that the fixed sample \mathcal{X} are drawn i.i.d.-ly from a probability distribution. Similarly, we have a distributional result as follows.

Theorem 4. In addition to the assumption in Theorem 3, we assume $P(|T_n - \theta_0| \le \eta) \to 1$ as $n \to \infty$ (for the "true" parameter values θ_0 formally defined on page 50), then the estimator T_n defined by

$$\frac{1}{\sqrt{n}} \sum_{i=1}^{n} \psi(x_i; T_n) \xrightarrow{n \to \infty} 0, a.s. P$$

would satisfy

$$\frac{1}{\sqrt{n}} \sum_{i=1}^{n} \psi(x_i; T_n) + \sqrt{n} \lambda(T_n) \xrightarrow{n \to \infty} 0, a.s. P$$

Particularly, our loss function would satisfy differentiability at θ_0 and $\sqrt{n}(T_n - \theta_0)$ is asymptotically normal with mean zero and covariance matrix

$$\left(\nabla_{\theta_0}\lambda^{-1}\right)\cdot\left(\left[\psi(x_i;\theta_0)-\mathbb{E}_P\psi(x_i;\theta_0)\right]^T\left[\psi(x_i;\theta_0)-\mathbb{E}_P\psi(x_i;\theta_0)\right]\right)\cdot\left(\nabla_{\theta_0}\lambda^{-1}\right)^T.$$

Proof. See Appendix
$$G.3$$
.

Relying on the geometric loss function \mathcal{L} , SRCA lost the analytic solution as in SPCA (Li et al., 2022). However, this geometric loss benefits the theoretic results state above, and can be replaced by other types of loss functions so that SRCA can be applied more widely.

We also assumed that the index set \mathcal{I} is fixed for our statements of theorems. In the exhaustive search, these results above can be applied individually to fixed \mathcal{I} ; but in the

 l_1 -relaxed problem 2.5, since the optimization is a joint optimization our asymptotic results Theorem 3 and 4 in this section do not apply.

4 Numerical Experiments

With theoretical results above on MSE, we also wish to see the practical performance of SRCA against the state-of-the-art dimension reduction methods on real datasets (we have already provided some performance illustration on synthetic datasets in Figure 2.1, see Appendices A and B for more examples.) We focus on the empirical structure preserving and coranking measurements below, and discuss the choice of parameters in SRCA in the end. The details of data selection are in Appendix D.

4.1 MSE

As a dimension reduction method, the most common and natural measurement of performance is based on the the mean squared error (MSE) between the original and reduced datasets measures how close the manifold is to the original observations. However, most dimension reduction methods only output low dimension features, like LLE, Isomap, tSNE, UMAP, GPLVM, etc, where the MSE is not well-defined because the low dimensional features cannot be trivially embedded into original data space \mathbb{R}^d . Algorithms that output projected data in the original space \mathbb{R}^d include SPCA, PCA, and our proposed SRCA, can be evaluated in terms of MSE.

We compare DR methods including PCA, SPCA and SRCA using MSE, on several real datasets whose detailed description of these dataset are in Appendix D.

Table 4.1 presents the MSEs of three competing algorithms on these datasets with $d' = \min\{d-1, 4\}$. The out-sample MSEs show a similar patterns and is postponed to the Appendix H. It is not hard to see that SRCA has the property of MSE minimization for most datasets and most d', as predicted by theory in Theorem 2.

The simplicity and elegance of SRCA is evidenced by the design of a geometric loss function, theory and experiment by this point. We would witness more of its power with respect to other metrics over real datasets below.

4.2 Cluster Preserving

Cluster structure properties of different dimension reduction algorithms varies, however, we hope that the data points belonging to the same group in the original dataset, would be close together in the dimension-reduced dataset.

Dataset	Method/d' =	1	2	3	4
	PCA	15.6261	6.3356	1.9479	
Banknote	SPCA	16.3717	8.1004	1.7348	
	SRCA	13.439	5.5088	1.0743	
Power	PCA	222.2971	55.4460	23.5173	2.9957
Plant	SPCA	162.8865	102.1006	45.5793	41.5251
	SRCA	150.8041	52.1439	19.8839	3.0373
User	PCA	0.1921	0.1253	0.0718	0.0311
Knowledge	SPCA	0.1465	0.0893	0.0477	0.0148
	SRCA	0.1458	0.0887	0.0471	0.0142
	PCA	0.076693	0.035222	0.020522	0.00756
Ecoli	SPCA	0.047776	0.032948	0.019648	0.01136
	SRCA	0.076660	0.032799	0.018332	0.00756
	PCA	6.7056	4.7711	3.3636	2.3218
Concrete	SPCA	5.4743	3.9934	2.9681	1.9181
	SRCA	5.4741	3.9909	2.9552	1.8985
	PCA	0.0245	0.0121	0.0059	0.0038
Leaf	SPCA	0.0155	0.0094	0.0072	0.0037
	SRCA	0.0230	0.0093	0.0054	0.0033
	PCA	1.4100	1.3204	1.2323	1.1450
Climate	SPCA	1.3563	1.2648	1.1781	1.0907
	SRCA	1.3554	1.2646	1.1780	1.0905

Table 4.1: MSE for different experiments.

For visualization, we fix retained dimension to be d'=2 and compare the following six algorithms: SRCA, SPCA, PCA, LLE, tSNE, UMAP. We choose these competitors to visualize in 2-dimensional figures, since they have the best practical performance on datasets we considered in this paper. To further quantify the performance, the Silhouette Score (SC, (Rousseeuw, 1987)), Calinski-Harabasz Index (CHI, (Caliński and Harabasz, 1974)) and Davis-Bouldin index (DBI, (Davies and Bouldin, 1979)) are considered. Higher SC and CHI, lower DBI imply better separation between clusters

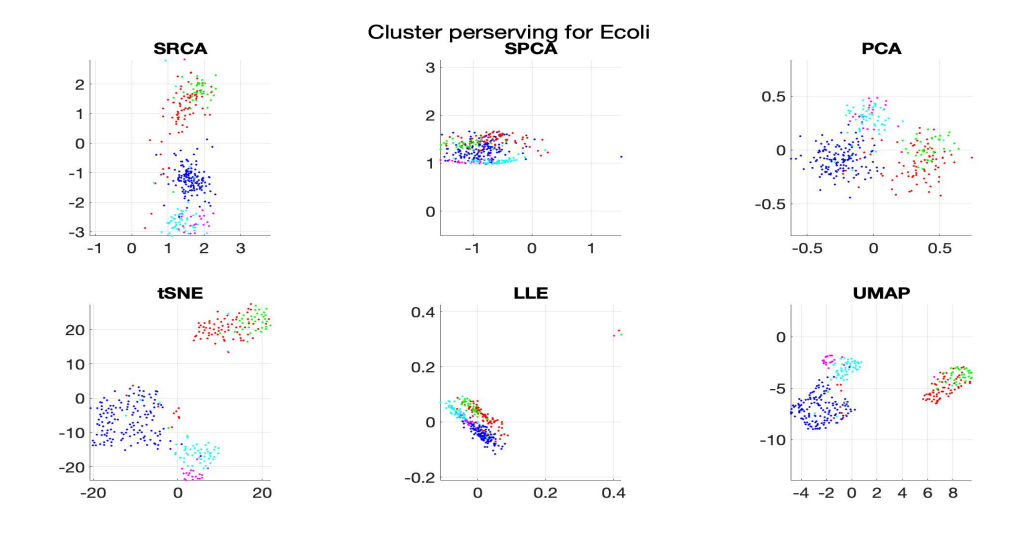


Figure 4.1: Cluster structures for Ecoli, d' = 2, there are five different clusters represented by different colors in the reduced dataset.

in the dataset. We provide these measures on the original labeled dataset (without any DR) as baselines. These indices computed on the dimension-reduced datasets would quantify how well the clustering structures are preserved after reduction.

Figure 4.1 and Table 4.2 show that SRCA outperforms SPCA, PCA and LLE in terms of all three metrics and is comparable to tSNE and UMAP, the state-of-the-art visualization algorithms designed fro d'=2. SRCA also has advantage over its predecessor SPCA and simpler linear method like PCA. With these experiments and the basic examples in Figure 1.1 and Appendix B, we conclude that if the dataset has strong spatial sphericity, we usually have good cluster preserving properties from SRCA. If the dataset is highly non-linear, tSNE and UMAP are usually better at the cost of creating fake clusters if tuning parameters are not well chosen (Wattenberg et al., 2016; Wilkinson and Luo, 2020).

Index	Baseline	SRCA	SPCA	PCA	LLE	tSNE	UMAP
\overline{SC}	0.257	0.267	0.260	0.200	0.209	0.293	0.290
CHI	133	192	190	215	46.6	376	376
DBI	1.49	1.59	1.58	2.56	2.40	1.37	1.32

Table 4.2: Clustering performance measures for Ecoli

4.3 Coranking Matrix

Another type of quantitative measures is based on the coranking matrix (Lee and Verleysen, 2009; Lueks et al., 2011). The coranking matrix can be viewed as the joint histogram of the ranks of original samples and the dimension-reduced samples. The coranking matrix can be used to assess results of dimension reduction methods. Entry q_{kl} in the coranking matrix is defined as $q_{kl} := \{(i,j) \mid \rho_{ij} = k \text{ and } r_{ij} = l\}$, where $\rho_{ij} := \{k : d(x_i, x_k) < d(x_i, x_j) \text{ or } d(x_i, x_k) = d(x_i, x_j), k < j\}$ stores the rank of the pair x_i, x_j in the original dataset; $r_{ij} := \{k : d(\hat{x}_i, \hat{x}_k) < d(\hat{x}_i, \hat{x}_j) \text{ or } d(\hat{x}_i, \hat{x}_k) = d(\hat{x}_i, \hat{x}_j), k < j\}$ stores the rank of the pair \hat{x}_i, \hat{x}_j in the dimension-reduced dataset.

The rank error is the difference between the original ranks ρ_{ij} and reduced ranks r_{ij} . We call the event of a nonzero rank error an *intrusion event*, where the rank pair reversed in the dimension-reduced dataset. An ideal dimension reduction method should preserves all the ranks of these pairwise distances between original and reduced datasets. That is, we have identical ordering of these pairwise distances in the original space and the dimension-reduced space. Coranking matrix is a finer analysis tool than the so-called ijk rank test (See, e.g., Solomon et al. (2021)).

We provide three scores (the higher the better) related to coranking matrices of the dimension-reduced results: CC (cophenetic correlation, measuring correlation between distance matrices), AUC (area under curve for the R_{NX} score), WAUC (weighted AUC) computed from coRanking R-package (Kraemer et al., 2018).

To understand our subsequent analyses better, we referred our readers to the analysis of the dimension reduction result of simple examples like \mathbb{S}^2 , \mathbb{T}^2 and a plane diffeomorphic to \mathbb{R}^2 , evaluated by these coranking matrix related scores in Appendix B, where SRCA is the only dimension method that consistently behaves almost the best in plane, spheres and topologically non-trivial examples like torus when measured by coranking scores. More coranking based experiments on real datasets are in Appendix E.

Another advantage of SRCA over existing DR methods is that it allows n < d', which happens to a variety of real datasets, specially for biomedical data where both d and d' are large. For example, in Genotype-Tissue Expression(GTEx) dataset (Consortium, 2020), some tissues are hard to collect so the the sample sizes are small but the dimension is very high, like Kidney Medulla (n = 4), Fallopian Tube (n = 9) and Cervix Endocervix (n = 10). However, there are thousands of genes so we expect that the intrinsic dimension d' > n. Following the common practice of feature selection in this database, we subsetted the data to the most variable 500 genes (Townes et al., 2019). Most competitors mentioned before are not directly applicable anymore when d' > n, including tSNE, UMAP, Isomap, MDS, etc. For illustration purpose, we retain

the first n dimensions. As a result, we present the three coranking based measurements on three tissues obtained from SRCA, SPCA, PCA and LLE for different d' in Figure 4.2.

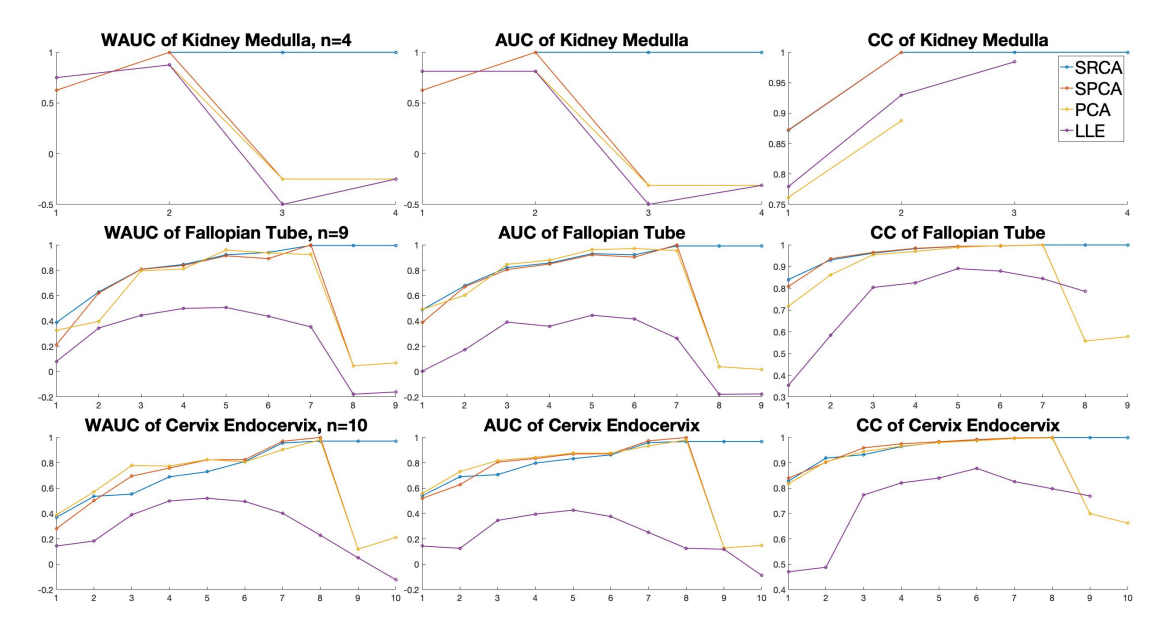


Figure 4.2: Coranking measurements of three GTEx tissues for different reduced dimension, the horizontal axes are retained dimension d', the vertical axes are score values.

From plots in Figure 4.2, we conclude that SRCA almost always outperforms SPCA, PCA and LLE in terms of coranking measures when d' < n. When d' > n, none of the competitors can be generalized easily to show performance that are comparable to SRCA, as expected.

4.4 Parameter Selection

In dimension reduction applications, there are usually certain tuning parameters . For classical DR methods, like PCA or MDS, the parameter usually has a explicit geometric interpretation. For modern nonlinear DR methods, like tSNE and UMAP, the parameters would affect both reproducibility and interpretability of the resulting dimension-reduced dataset.

It is a separate but important problem how we could select (or tune) the parameter of both classical and modern dimension reduction methods. However, we shall discuss the effect of three parameters in SRCA in this section. Unlike tSNE or UMAP, SRCA has the advantage of being parsimonious in parameterization, while each of its parameters

is highly interpretable. We study the problem of prarmeter selection for SRCA in this section.

4.4.1 Retained dimension d'

The first parameter that dictates the behavior of most DR methods is the retained dimension d' (see the remark on page 4), which can be determined by subsequent purpose (e.g., the tSNE and UMAP usually take d' = 2,3 for visualizations). When the practitioner is unsure about the choice of d', there is a trade-off between retained information and reduction of dimensionality. For linear DR methods like PCA, we usually use the residual norms (i.e., the total variance minus explained variance) to decide d'. Multiple cautionary notes (Jolliffe, 1982) have pointed out that such a straightforward selection of principal components based purely on the magnitude of eigenvalues could be problematic.

In our method SRCA, the d' is selected based on MSE computed from a non-linear distance function. Besides its non-linear nature, we tie the criterion back to the geometric nature of the dataset. Therefore, we expect this criteria would naturally preserve distances and clustering induced by geometry. We also note that the MSE-based criteria is a benefit of approximating the manifold in the original space (SRCA, SPCA, PCA), instead of a new space (LLE, tSNE, etc).

4.4.2 Rotation methods

The second parameter is the choice of rotation methods, which is highly data dependent and would affect the clustering and visualization most. Regarding the MSE performance, Table 4.3 investigates the performance of SRCA with different kinds of rotations. We can see that the PCA rotation usually give a reasonable result in terms of MSE performance. Both PCA and quartimax rotations used along with SRCA method would outperform dimension reduction of PCA and SPCA separately. We have similar observations for some other datasets with n > d (e.g., Leaf, PowerPlant, etc., see Appendix D).

The choice of rotation methods could also be made to accommodate the type of noise in observations. In the situation where the tail behavior of the noise is close to Gaussian and the W is known (or, by default I), PCA is our default choice; but in the situation where the noise is non-Gaussian and we do not have much knowledge for W, then ICA (Hyvärinen and Oja, 2000) is probably a better option.

Based on the empirical evidence obtained from real datasets (e.g., Table 4.3), we recommend using PCA rotation as a default, but other types of rotations can be useful

for specific datasets, if desired (Jolliffe, 1995).

	PCA	SPCA				SRCA			
$\overline{d'}$			PCA	varimax	orthomax	quartimax	equamax	parsimax	ICA
1	15.6	16.4	13.4	18.4	18.5	14.9	27.5	26.6	14.5
2	6.34	8.10	5.51	6.19	6.19	5.79	13.2	13.4	5.36
3	1.95	1.73	1.07	1.07	1.07	1.07	1.07	1.07	1.14

Table 4.3: MSE of Banknote (see AppendixD) for different rotation methods in the SRCA procedure. We also include two other DR methods PCA and SPCA to compare against SRCA. The first row records the DR methods (PCA, SPCA and SRCA); the second row records the optimal rotation method used by SRCA.

4.4.3 Sparse penalty parameter λ

The third parameter we want to consider is the penalty parameter λ that controls the retained dimension d' when l_1 approximation is in place as defined in (2.8). When a strict binary search like l_0 optimization in (2.5) is used, the penalty is usually not needed. However, the caution we shall take here is that the selection of sparsity penalty parameter λ should roughly be at the same magnitude as the loss function in order to function properly.

The tuning parameter $\lambda > 0$ would be part of the the objective function instead of constraints. In some applications, the penalty term can also be replaced with $\lambda \sum_{i=1}^{n} \|I_{\mathcal{I}}x_i\|_1$. In experiments, we found that SRCA is not sensitive to λ ; In very high-dimensional datasets (e.g., Alon (see Appendix D), GTEx), the choice of this parameter would also affect the convergence speed in the execution of the optimization algorithm, a larger penalty parameter would force the numerical algorithm converge slightly faster. Alternatively, we can also treat the choice of this parameter as a apriori tuning parameter of the loss function, whose values can be selected for different datasets using cross-validation.

λ	10^{-1}	10^{-2}	10^{-3}	10^{-4}	10^{-5}	0
$\overline{\text{CC}}$	0.704	0.727	0.730	0.730	0.730	0.730
AUC	0.408	0.416	0.416	0.416	0.416	0.416
WAUC	0.261	0.256	0.256	0.256	0.256	0.256

Table 4.4: Coranking performance scores for different λ 's on the Alon dataset, d'=2.

4.5 Observations

We organize the observations from above experiments in sections 4.1 to 4.4 as the following list:

- 1. When the retained dimensions $d' < \min\{d, n\}$,
- (a) SRCA behaves very similarly to SPCA in terms of the MSE, both outperform PCA alone across different real datasets. The interesting observation is that SRCA outcompetes both of them in some simple but geometrically nontrivial examples like the ones in Appendix B.
- (b) SRCA behaves differently from SPCA and PCA in terms of preserving clustering structures. Although SRCA cannot always outperform the methods that are designed for cluster structure preserving (e.g., tSNE, UMAP), it outperforms PCA and SPCA.
- 2. When $d > d' \ge n$, the SRCA outperforms PCA, SPCA and other nonlinear DR methods in terms of the coranking scores across different real datasets. Only SRCA yields consistently better dimension reduction results when d' < n and $d' \ge n$.
- 3. SRCA is the slowest in terms of computational time among SRCA, SPCA and PCA. But it is rather fast compared to some non–linear methods like Isomap.
- (a) For rather low-dimensional original dataset ($d \le 10$), a brute-force solution of the SRCA is acceptable.
- (b) For moderate dimensional original dataset ($d = 10 \sim 100$), our proposed l_1 approximating approach of the SRCA is efficient and reasonably accurate.
- (c) For high-dimensional original dataset ($d \ge 100$), our SRCA method would also suffer from the matrix factorization cost used in PCA.
 - i. We can introduce sparse PCA to take the sparsity into account.
 - ii. We can introduce randomized PCA to speed up the computation.

5 Conclusion

5.1 Contribution

In this paper, we propose a novel DR method by proposing a PCA-induced rotation with a geometric induced loss function that minimizes MSE between the original and reduced datasets. Our motivation is to get the dimension reduction for spherical datasets (or datasets with spherical and elliptical structures) to respect the geometry in the original space. Its variant also works with a general weight matrix W and sparsity penalty λ . This is a statistically principled way with asymptotic theoretic guarantee.

Unlike traditional DR methods like PCA and MDS, SRCA works smoothly with a stable performance even when $d \geq d' + 1 > n$ which is extremely important in biomedical data DR, especially in gene expression data (e.g.,GTEx). Accompanying generalized algorithms for SRCA are also developed, with detailed convergence and a straightforward parallel potentiality for real-world practice. SRCA is related to PCA and SPCA but also generalizes the former into a spherical setting and the latter one into a one-step procedure. Most importantly, SRCA removes the d' < n requirements in these predecessors in a unified framework using novel loss functions.

Compared to non-linear methods, SRCA has geometrical interpretation and practical convenience. Its unique binary search also allows parallelizations when applied to big datasets. A comprehensive experimental study of SRCA against a collection of state-of-art DR methods has been done with detailed qualitative and quantitative measures, revealing the superiority of SRCA.

To sum up, we provide a principled way that targets at an explicitly designed geometric loss function and provide an algorithm along with statistical guarantees and a comprehensive evaluation of this novel DR method.

5.2 Discussions and Future Works

In this paper, we propose a new method designed for dimension reduction for spherical datasets. We also provide simulated and real-world data analysis along with theoretic discussions to support our findings that our SRCA method minimizes the point-to-sphere distance by the design of a loss function. Empirical experiments with detailed quantitative comparisons also show that it preserved the clustering structures. In addition, SRCA can be relaxed through a sparsity penalty term.

Our current technique focuses on but is not limited to the spherical dataset. Similar designs of loss functions can be generalized to a wider variety of spaces like symmetric spaces (Li et al., 2020) using multivariate decomposition technique like ICA, and a wider range of datasets like binary datasets (Landgraf and Lee, 2020).

DR methods that do not incorporate the information of the global geometry or topology well enough would lead to the problematic results (Figure 1.1). Although topology-based statistics has been proposed to describe this aspect of the dimension reduction problem (Solomon et al., 2021), it is also not clear at the moment how geometry and topology can interplay with each other in the context of dimension reduction (Luo et al., 2021; Luo and Strait, 2019). In the current paper, the loss function is a summation of functions in the form of $u(x_i, \theta)$ with the parameters θ being the center c, radius r and the selected subspace. It is also more general than the least-square approach

(Suzuki and Sugiyama, 2010) since SRCA does not need probability assumptions to work, but behaves well when stochastic noises are involved.

The geometric loss function has some relation to or is motivated by the statistical problem we are trying to solve. Then the reduced dataset should be more suitable for the subsequent statistical method to be applied. In terms of DR research, we point out and give a partial solution to a problem in the research by various novel examples in the text (i.e., Appendices A and B): how should we respect the geometry and/or topology of the underlying space when performing DR or subsequent statistical problem?

There are several directions of future work that we wish to pursue:

- 1. Generalize the methodology of SRCA to other manifolds other than spheres like the topologically non-trivial tori. In addition, we also hope to develop a localized version of SRCA that can be applied to a wider range of manifolds with locally spherical structures. It is attractive to develop a kernelized generalization to the SRCA method like kernel PCA proposed by Schölkopf et al. (1997) to handle more complicated structure than spherical datasets. It is likely that for manifold with interesting local behaviors, a localized version of SRCA like Li et al. (2022) would be beneficial.
- 2. Investigation of loss functions induced by different kinds of geometric characteristics. We wish to investigate a mixed version of two (or more) different geometrically induced loss functions and the trade-off between two (or more) distinct geometric features during the dimension reduction (Luo et al., 2021), using the loss function in the form $u_h(x_i, \theta_h)$ governed by the shared latent parameter h (Luenberger et al., 1984).

Following our framework in the current paper, we suggest a different approach of minimizing the $\sum_{x \in S \subset X} d_{W,I}(\psi(x), \pi_S(x))$ directly as shown in (2.3) and does not require a discretization of the dataset.

- 3. Visualization using SRCA. We expect to use SRCA for visualization and exploratory data analysis with consistency results like the results in the sense of Johnstone and Lu (2009). Besides the theoretic study of sparsity in high-dimensional dataset, parallel computations for the binary search in high-dimensional datasets is of practical interest. Especially when both n and d are high and when d' + 1 exceeds n, PCA and SPCA fail but SRCA still works with optimal rotations. It is of great interest to see how geometric or topological loss function DR methods perform in data visualization.
- 4. Statistical dimension reduction with a topologically induced loss function, where the distributed persistence serves as a statistics that aids dimension reduction (section VI in Solomon et al. (2021)).
- 5. Efficient randomized implementation with theoretical guarantees. Note that the

novel formulation (2.8) of our DR method falls into a special case of "weighted low-rank" approximation problems (Razenshteyn et al., 2016; Srebro and Jaakkola, 2003), this leads us to a possible future direction of leveraging the power of numerical linear algebraic algorithms in SRCA. We expect that this would allow us to perform DR methods on much larger datasets.

Acknowledgement

HL wants to thank Dmitriy Morozov, Leland Wilkinson for motivating discussions and comments. HL was supported by the Director, Office of Science, of the U.S. Department of Energy under Contract No. DE-AC02-05CH11231., who wants to thank the support of LBNL CRD during this research. DL wants to thank David Dunson for motivating discussions.

Our code for SPCA, SRCA implementations and experiments are publicly available at http://www.github.com/hrluo/SRCA.

References

- Alon, U., N. Barkai, D. Notterman, K. Gish, S. Ybarra, D. Mack, and A. Levine (1999). Broad patterns of gene expression revealed by clustering analysis of tumor and normal colon tissues probed by oligonucleotide arrays. *Proceedings of the National Academy of Sciences* 96(12), 6745–6750.
- Banerjee, A., I. Dhillon, J. Ghosh, and S. Sra (2003). Generative model-based clustering of directional data. In *Proceedings of the ninth ACM SIGKDD international conference on Knowledge discovery and data mining*, pp. 19–28.
- Banerjee, A., I. S. Dhillon, J. Ghosh, S. Sra, and G. Ridgeway (2005). Clustering on the unit hypersphere using von mises-fisher distributions. *Journal of Machine Learning Research* 6(9).
- Boyd, S., S. P. Boyd, and L. Vandenberghe (2004). *Convex optimization*. Cambridge university press.
- Boyd, S., L. Xiao, and A. Mutapcic (2003). Subgradient methods. *lecture notes of EE392, Stanford University, Autumn Quarter 2004*, 2004–2005.
- Caliński, T. and J. Harabasz (1974). A dendrite method for cluster analysis. Communications in Statistics-theory and Methods 3(1), 1–27.

- Chernov, N. (2010). Circular and linear regression fitting circles and lines by least squares. Taylor & Francis.
- Consortium, G. (2020). The gtex consortium atlas of genetic regulatory effects across human tissues. *Science* 369 (6509), 1318–1330.
- Davies, D. L. and D. W. Bouldin (1979). A cluster separation measure. *IEEE transactions on pattern analysis and machine intelligence* (2), 224–227.
- Doob, J. L. (1953). Stochastic processes, Volume 10. Wiley: New York.
- Dryden, I. L. et al. (2005). Statistical analysis on high-dimensional spheres and shape spaces. The Annals of Statistics 33(4), 1643–1665.
- Erichson, N. B., P. Zheng, K. Manohar, S. L. Brunton, J. N. Kutz, and A. Y. Aravkin (2020). Sparse principal component analysis via variable projection. *SIAM Journal on Applied Mathematics* 80(2), 977–1002.
- Huber, P. J. (2004). Robust statistics, Volume 523. John Wiley & Sons.
- Huber, P. J. et al. (1967). The behavior of maximum likelihood estimates under non-standard conditions. In *Proceedings of the fifth Berkeley symposium on mathematical statistics and probability*, Volume 1, pp. 221–233. University of California Press.
- Hyvärinen, A. and E. Oja (2000). Independent component analysis: algorithms and applications. *Neural networks* 13(4-5), 411–430.
- Johnstone, I. M. and A. Y. Lu (2009). On consistency and sparsity for principal components analysis in high dimensions. *Journal of the American Statistical Association* 104 (486), 682–693.
- Jolliffe, I. T. (1982). A note on the use of principal components in regression. *Journal* of the Royal Statistical Society: Series C (Applied Statistics) 31(3), 300–303.
- Jolliffe, I. T. (1995). Rotation of principal components: choice of normalization constraints. *Journal of Applied Statistics* 22(1), 29–35.
- Jolliffe, I. T. and J. Cadima (2016). Principal component analysis: a review and recent developments. *Philosophical Transactions of the Royal Society A: Mathematical, Physical and Engineering Sciences* 374 (2065), 1–16.

- Journée, M., Y. Nesterov, P. Richtárik, and R. Sepulchre (2010). Generalized power method for sparse principal component analysis. *Journal of Machine Learning Research* 11(2).
- Kraemer, G., M. Reichstein, and M. D. Mahecha (2018). dimred and coranking—unifying dimensionality reduction in r. R Journal 10(1), 342–358.
- Kruskal, J. B. (1978). Multidimensional scaling. Number 11. Sage.
- Landgraf, A. J. and Y. Lee (2020). Dimensionality reduction for binary data through the projection of natural parameters. *Journal of Multivariate Analysis* 180, 104668.
- Lee, J. A. and M. Verleysen (2009). Quality assessment of dimensionality reduction: Rank-based criteria. *Neurocomputing* 72(7-9), 1431–1443.
- Li, D., Y. Lu, E. Chevalier, and D. B. Dunson (2020). Density estimation and modeling on symmetric spaces. arXiv preprint arXiv:2009.01983.
- Li, D., M. Mukhopadhyay, and D. B. Dunson (2022). Efficient Manifold Approximation with Spherelets. *Journal of the Royal Statistical Society: Series B (Statistical Methodology)*.
- Lueks, W., B. Mokbel, M. Biehl, and B. Hammer (2011). How to evaluate dimensionality reduction?—improving the co-ranking matrix. arXiv preprint arXiv:1110.3917.
- Luenberger, D. G., Y. Ye, et al. (1984). *Linear and nonlinear programming*, Volume 2. Springer.
- Luo, H., J. Kim, A. Patania, and M. Vejdemo-Johansson (2021). Topological learning for motion data via mixed coordinates. *The IEEE International Conference on Big Data (IEEE BigData 2021)*, 1–6.
- Luo, H., S. N. MacEachern, and M. Peruggia (2020). Asymptotics of lower dimensional zero-density regions. *arXiv:2006.02568*, 1–28.
- Luo, H., A. Patania, J. Kim, and M. Vejdemo-Johansson (2021). Generalized penalty for circular coordinate representation. *Foundations of Data Science*, 1–37.
- Luo, H. and J. Strait (2019). Combining geometric and topological information in image segmentation. arXiv preprint arXiv:1910.04778.
- McInnes, L., J. Healy, N. Saul, and L. Grossberger (2018). Umap: Uniform manifold approximation and projection. *The Journal of Open Source Software* 3(29), 861.

- Mukhopadhyay, M., D. Li, and D. B. Dunson (2020). Estimating densities with non-linear support by using fisher–gaussian kernels. *Journal of the Royal Statistical Society: Series B (Statistical Methodology)* 82(5), 1249–1271.
- Pearson, K. (1901). On lines and planes of closest fit to systems of points in space. The London, Edinburgh, and Dublin Philosophical Magazine and Journal of Science 2(11), 559–572.
- Razenshteyn, I., Z. Song, and D. P. Woodruff (2016). Weighted low rank approximations with provable guarantees. In *Proceedings of the forty-eighth annual ACM symposium on Theory of Computing*, pp. 250–263.
- Rousseeuw, P. J. (1987). Silhouettes: a graphical aid to the interpretation and validation of cluster analysis. *Journal of computational and applied mathematics* 20, 53–65.
- Roweis, S. T. and L. K. Saul (2000). Nonlinear dimensionality reduction by locally linear embedding. *science* 290(5500), 2323–2326.
- Schölkopf, B., A. Smola, and K.-R. Müller (1997). Kernel principal component analysis. In *International conference on artificial neural networks*, pp. 583–588. Springer.
- Schölkopf, B., A. Smola, and K.-R. Müller (1998). Nonlinear component analysis as a kernel eigenvalue problem. *Neural computation* 10(5), 1299–1319.
- Schubert, E. and M. Gertz (2017). Intrinsic t-stochastic neighbor embedding for visualization and outlier detection. In *International Conference on Similarity Search and Applications*, pp. 188–203. Springer.
- Solomon, E., A. Wagner, and P. Bendich (2021). From geometry to topology: Inverse theorems for distributed persistence. arXiv preprint arXiv:2101.12288.
- Srebro, N. and T. Jaakkola (2003). Weighted low-rank approximations. In *Proceedings* of the 20th International Conference on Machine Learning (ICML-03), pp. 720–727.
- Suzuki, T. and M. Sugiyama (2010). Sufficient dimension reduction via squared-loss mutual information estimation. In *Proceedings of the Thirteenth International Con*ference on Artificial Intelligence and Statistics, pp. 804–811. JMLR Workshop and Conference Proceedings.
- Tenenbaum, J. B., V. De Silva, and J. C. Langford (2000). A global geometric framework for nonlinear dimensionality reduction. *science* 290 (5500), 2319–2323.

- Titsias, M. and N. D. Lawrence (2010). Bayesian gaussian process latent variable model. In *Proceedings of the Thirteenth International Conference on Artificial Intelligence and Statistics*, pp. 844–851. JMLR Workshop and Conference Proceedings.
- Townes, F. W., S. C. Hicks, M. J. Aryee, and R. A. Irizarry (2019). Feature selection and dimension reduction for single-cell rna-seq based on a multinomial model. *Genome biology* 20(1), 1–16.
- Van der Maaten, L. and G. Hinton (2008). Visualizing data using t-sne. *Journal of machine learning research* 9(11).
- Wattenberg, M., F. Viégas, and I. Johnson (2016). How to use t-sne effectively. Distill.
- Wilkinson, L. and H. Luo (2020). A Distance-preserving Matrix Sketch. arXiv:2009.03979.
- Zhang, L., T. Dunn, J. Marshall, B. Olveczky, and S. Linderman (2021). Animal pose estimation from video data with a hierarchical von mises-fisher-gaussian model. In *International Conference on Artificial Intelligence and Statistics*, pp. 2800–2808. PMLR.

Appendices

A Orthogonal Loop Examples

We consider the original dataset shown in Figure 1.1 again, but each coordinates is perturbed by a Gaussian noise with mean zero and different noise variances. As the noise variance increases, we observe that the topological structure of this example of two orthogonal loops becomes less and less obvious. We can see that SRCA is consistently achieving the lowest matched MSE defined in Section 4.1, while both SPCA and SRCA preserves the topological structure relatively well. In Table A.1, we provide MSE for more settings of noise variances to show the MSE from each different DR methods. It can be observed that PCA becomes worse quickly in terms of MSE.

Noise Var.	0	0.01	0.05	0.10	0.20	0.40	1.00
PCA	0.24750	0.24889	0.25634	0.26990	0.31126	0.45045	1.2653
SRCA	0.10408	0.10421	0.10623	0.11237	0.13668	0.21834	0.64711
SPCA	0.12758	0.12764	0.12925	0.13448	0.15585	0.22861	0.65268

Table A.1: MSE for different DR methods performed on the same orthogonal loop dataset but with different noise variances in the Gaussian perturbation.

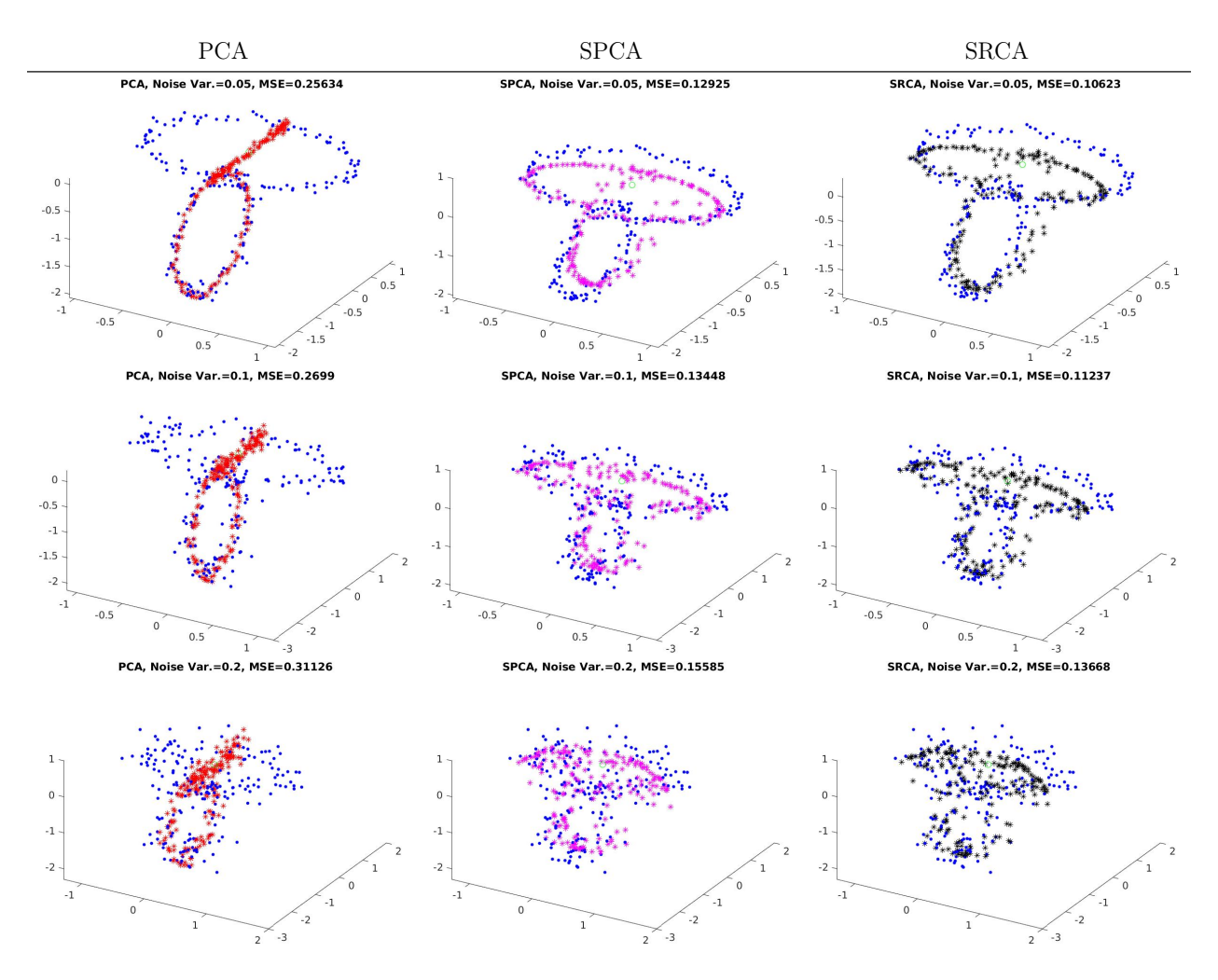


Figure A.1: On the left columns we show the original dataset in blue points, and the PCA dimension-reduced dataset in red stars. On the middle column we show the original dataset in blue points, and the SPCA dimension-reduced dataset in magenta stars. On the right column we show the original dataset in blue points, and the SRCA dimension-reduced dataset in black stars.

B Other Basic Examples

In this appendix, we consider several basic examples we use to illustrate the difference between PCA, SRCA, and SPCA. Below, we provide the quantitative measures for each of these examples and the coranking summaries. In (a) plane, we uniformly sample points $(x_1, x_2, 0)$ from $[-3, 3] \times [-3, 3] \times \{0\}$. In (b) torus, we take the parameterization

$$((R_1 + R_2 \cos \theta) \cos \phi, (R_1 + R_2 \cos \theta) \sin \phi, R_2 \sin \theta)$$

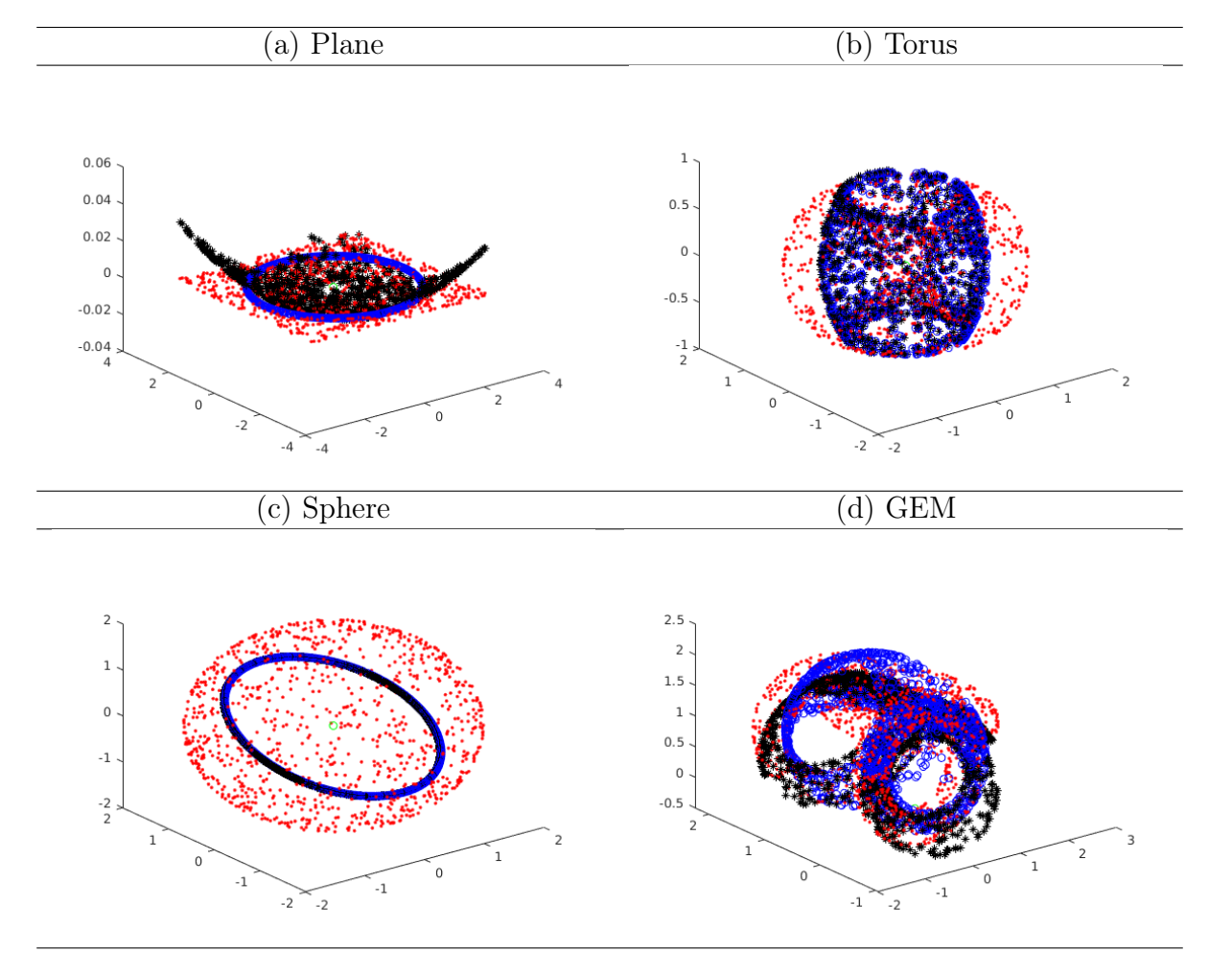


Figure B.1: The datasets for the basic example. In these examples the datasets are observed in \mathbb{R}^3 (d=3) and we want to reduce the dataset by one dimension (d'=2). In each of the above panels, the red solid dots are the original datasets sampled from a uniform distribution lying on (a) plane (b) torus (c) sphere (d) triple torus without interior intersection (GEM). The blue circles are the points in reduced dataset obtained by SPCA. The black stars are the points in reduced dataset obtained by SRCA. We do not display the result of PCA in these figures.

where $R_1 = 1/2$ and $R_2 = 1/3$. The parameters (θ, ϕ) are uniformly sampled from $[0, 2\pi) \times [0, 2\pi)$. In (c) sphere, we take the canonical parameterization and uniform sampling on the parameter space $[0, 2\pi) \times [0, 2\pi)$, which is equivalent to von-Mises Fisher distribution with concentration $\kappa = 0$. In (d) triple torus, we independently sampled 3 batches of points with equal sample sizes. Then we multiply each of these 3

batches with the following rotation matrices and add a translation vector:

$$R_{1} = \begin{pmatrix} 1 & 0 & 0 \\ 0 & \cos\frac{\pi}{2} & -\sin\frac{\pi}{2} \\ 0 & \sin\frac{\pi}{2} & \cos\frac{\pi}{2} \end{pmatrix}, \tau_{1} = \begin{pmatrix} 0 \\ 0 \\ 3 \end{pmatrix}.$$

$$R_{2} = \begin{pmatrix} \cos\frac{\pi}{4} & 0 & \sin\frac{\pi}{4} \\ 0 & 1 & 0 \\ -\sin\frac{\pi}{4} & 0 & \cos\frac{\pi}{4} \end{pmatrix}, \tau_{2} = \begin{pmatrix} 0 \\ 3 \\ 3 \end{pmatrix}.$$

$$R_{3} = \begin{pmatrix} \cos 0 & -\sin 0 & 0 \\ \sin 0 & \cos 0 & 0 \\ 0 & 0 & 1 \end{pmatrix}, \tau_{3} = \begin{pmatrix} 3 \\ 3 \\ 3 \end{pmatrix}.$$

The resulting dataset contains three tori, and it is not difficult to verify that these three tori do not have interior intersections. We scale the dataset by subtracting $(1, 1, 1)^T$ from each point and multiply 1/2 entry-wisely.

	SRCA	SPCA	PCA	$_{ m LLE}$	tSNE	UMAP
$\overline{\text{CC}}$	0.9999998	0.9998008	1.0000000	0.9983610	0.9774094	0.9906862
AUC	0.9995782	0.9898617	0.9998370	0.9604653	0.8670743	0.9094597
WAUC	0.9990011	0.9913487	0.9991016	0.9725947	0.8460439	0.8320849

Table B.1: Performance scores and the coranking of plane.

		SRCA	SPCA	PCA	LLE	tSNE	UMAP
\overline{CC}	7	0.8222110	0.8208433	0.9777033	0.9751233	0.8523848	0.9072153
AU	С	0.6217176	0.6194763	0.8317488	0.8251250	0.6344541	0.7257927
WAU	JC	0.6025524	0.6033849	0.6104916	0.6092178	0.7430941	0.6707993

Table B.2: Performance scores and the coranking of torus.

	SRCA	SPCA	PCA	LLE	tSNE	UMAP
$\overline{\text{CC}}$	1.0000000	1.0000000	0.8026803	0.7262926	0.6762080	0.6810310
AUC	0.9999992	1.0000000	0.5585561	0.4876606	0.5171233	0.5696564
WAUC	0.9999998	1.0000000	0.4953096	0.4792300	0.7312668	0.7270227

Table B.3: Performance scores and the coranking of sphere.

	SRCA	SPCA	PCA	LLE	tSNE	UMAP
$\overline{\text{CC}}$	0.9986899	0.7407685	0.9987456	0.9963411	0.5697951	0.9438497
AUC	0.9509051	0.5618742	0.9518870	0.9205247	0.4646542	0.8042776
WAUC	0.7067388	0.5204686	0.7057702	0.6973970	0.7077429	0.6735852

Table B.4: Performance scores and the coranking of GEM.

From the performance evaluation table above, we can see that:

- 1. In the plane example, all linear and non-linear DR methods performs well in terms of performance evaluation measures and coranking summaries.
- 2. In the torus example, neither SPCA nor SRCA perform as good as other DR methods in terms of scores. However, in the visualization of the reduced dataset, we can see that both SPCA and SRCA preserve the structure of torus pretty well.
- 3. In the sphere example, both SPCA and SRCA give almost identical results, outperforming both the simplest PCA and the more sophisticated non-linear DR methods like tSNE and UMAP. In the visualization of the reduced dataset, we can see that both SPCA and SRCA reduce the data points on the sphere (d=3) to points on a geodesic circle (d'=2). This preserves the spherical nature of the dataset and yield a better result.
- 4. In the GEM example, the SRCA is the best in terms of almost all performance scores. A visual verification also reveals that the resulting reduced dataset preserves all three holes in the tori.

C SRCA Algorithms

In this section, we present the algorithm that solves our optimization problem (2.3) and (2.4). Algorithm 1 delineates the binary search strategy which exhausts 2^d possible subsets of $\{1, \dots, d\}$ to find an optimal subspace. Algorithm 2 delineates the l_1 -relaxation strategy which formulates the original problem (2.3) into an optimization problem (2.4) to find an optimal subspace.

Detailed explanation of algorithms in this section is as follows.

1. (Step 1: Get the empirical mean for \mathcal{X} .) Estimate the empirical mean $\bar{\mathcal{X}}$ for the dataset \mathcal{X} in \mathbb{R}^d , and subtract the mean $\bar{\mathcal{X}}$ to make sure that the assumption of

PCA is satisfied.

$$z_i = x_i - \frac{1}{n} \sum_{i=1}^n x_i = x_i - \bar{x}$$

2. (Step 2: Conduct the rotation.) We choose a rotation method to construct rotation matrix R based on the datset \mathcal{X} . Then we rotate the dataset \mathcal{X} to standard position $(\mathcal{X} - \bar{\mathcal{X}})R$. Here we use a chosen rotation matrix R (PCA, ICA or other kinds of optimal rotation) to rotate the sphere so that all its axes are parallel to the coordinate axes.

For PCA rotation, let the covariance matrix $cov(z_i) = R\Lambda R^T$ where Λ is diagonal and the rotation matrix R is orthogonal.

$$y_i = Rz_i$$

3. (Step 3: Binary search for the best d'+1 axes.) In this step we perform dimension reduction. Now that we can assume that the axes of the sphere (or ellipsoid) are parallel to the coordinate axes. We solve the binary optimization problem (2.3) with W=I (or other W if extremely skewed dataset is observed) to choose the optimal directions to retain. In this step we would find the optimal $v_{\rm opt}$ and hence the optimal index set $\mathcal{I}_{\rm opt}$.

In this optimization problem, as we stated in (2.3) above, we conduct dimension reduction by minimizing the loss function based on the point-to-ellipsoid distance to the estimated sphere $S_{\mathcal{I}}$.

The optimization problem is spelled out as (2.5).

- 4. (Step 4: Eliminate the un-chosen dimensions.) This simply sets drop the un-selected dimension not in \mathcal{I}_{opt} , equivalently, we find the v_{opt} in the notation of problems (2.3) and (2.4).
 - (a) In the standard form (2.3), we may let $\eta = v_{\text{opt}}$ be the binary vector such that $||v_{\text{opt}}||_{l_0} = d' + 1$.
 - (b) In the l_1 -relaxed form (2.4), the v_{opt} would have l_1 -norm less or equal than d'+1 but not binary entries. We construct a binary vector η such that only the first leading d'+1 entries with largest absolute values in v_{opt} are 1; and the rest entries are 0.
- 5. (Step 5: Re-estimate the center and radius.) Only in the problem (2.4), we re-estimate the center c_{opt} and radius r_{opt} using the same loss function but a fixed v_{opt} . In standard problem (2.3), we use the center c_{opt} and radius r_{opt} from step 3.

6. (Step 6: Project and rotate the sphere back into full space.) After we choose the dimension and axes, we project the dataset onto a sphere with the center c_{opt} and radius r_{opt} and add back the empirical mean $\bar{\mathcal{X}}$. More specifically, we project the datapoints x_i to the sphere S(c,r) as in (2.6) and then we simply we rotate the resulting dimension-reduced dataset back, using the inverse of the same rotation matrix R.

Algorithm 1: SRCA dimension reduction algorithm

Data: X (data matrix consisting of n samples in \mathbb{R}^d)

Input: d' (the dimension of the sphere), W (the covariance weight matrix, by default $W = I_d$), λ (optional, the sparse penalty parameter), rotationMethod (the method we use to construct the rotation matrix).

Result: \hat{c} (The estimated center of $S_{\mathcal{I}}$ in \mathbb{R}^d), \hat{r} (The estimated radius of $S_{\mathcal{I}}$), \mathcal{I}_{opt} (The optimal index subset)

GetRotation (X,rotationMethod) obtains a $d \times d$ rotation matrix based on the data matrix X. The rotationMethod option specifies what method we use to construct the rotation matrix, by default, we use PCA to obtain a rotation matrix.

ProjectToSphere (X,c,r,k) is a projection that projects the point set X onto an l_k -sphere of center c and radius r via $X \mapsto c + \frac{X-c}{\|X-c\|_{l_k}} \cdot r$.

```
1 begin
```

end

```
Standardize the dataset by subtracting its empirical mean X = X - \bar{X}
  2
            Construct a rotate matrix R = GetRotation (X, rotationMethod)
  3
            X_{rotated} = X * R
  4
            \mathcal{L}_{opt} = \infty
  5
            while \mathcal{I} \subset 1, \cdots, p do
                   Solve the optimization problem (2.3) with respect to c, r with a fixed \mathcal{I}
  6
                   Denote the solution as c_{cur}, r_{cur}, \mathcal{I}_{cur}
                  if \mathcal{L}(c, r, \mathcal{I} \mid \mathcal{X}) \leq \mathcal{L}_{opt} then
\mathcal{L}_{opt} \leftarrow \mathcal{L}(c, r, \mathcal{I} \mid \mathcal{X})
c_{opt} \leftarrow c_{cur}
r_{opt} \leftarrow r_{cur}
\mathcal{I}_{opt} \leftarrow \mathcal{I}_{cur}
            Construct the binary index vector \eta = (\eta_i), \eta_i = 1 iff i \in \mathcal{I} and \eta_i = 0 otherwise.
 8
            \hat{c} = c_{opt} \cdot \eta * R^{-1} + \bar{X}
            \hat{r} = r_{opt}
10
            X_{rotated}(:,\mathcal{I}) \leftarrow 0
11
            X_{rotated} \leftarrow \texttt{ProjectToSphere} \ (X, \hat{c}, \hat{r}, k)
12
            X_{output} \leftarrow X_{rotated} * R^{-1} + \bar{X}
13
```

Algorithm 2: SRCA dimension reduction algorithm with l_1 relaxation

Data: X (data matrix consisting of n samples in \mathbb{R}^d)

Input: d' (the dimension of the sphere), W (the covariance weight matrix, by default $W = I_d$), λ (optional, the sparse penalty parameter), rotationMethod (the method we use to construct the rotation matrix).

Result: \hat{c} (The estimated center of $S_{\mathcal{I}}$ in \mathbb{R}^d), \hat{r} (The estimated radius of $S_{\mathcal{I}}$), \mathcal{I}_{opt} (The optimal index subset)

GetRotation (X,rotationMethod) obtains a $d \times d$ rotation matrix based on the data matrix X. The rotationMethod option specifies what method we use to construct the rotation matrix, by default, we use PCA to obtain the rotation matrix.

ProjectToSphere (X,c,r,k) is a projection that projects the point set X onto an l_k -sphere of center c and radius r via $X \mapsto c + \frac{X-c}{\|X-c\|_{l_k}} \cdot r$.

```
1 begin
```

```
Standardize the dataset by subtracting its empirical mean X = X - \bar{X}
```

- 3 Construct a rotate matrix R = GetRotation(X, rotationMethod)
- 4 $X_{rotated} = X * R$
- Solve the optimization problem (2.4) with respect to c, r and v
- **6** Denote the solution as c_0, r_0, v_{opt}
- 7 Construct \mathcal{I} that contains the largest/leading d'+1 coordinates of v_{opt} .
- 8 Solve the optimization problem (2.3) with respect to c, r with a fixed \mathcal{I}
- 9 Denote the solution as c_{opt}, r_{opt}
- 10 $\hat{c} = c_{opt} \cdot \eta * R^{-1} + \bar{X}$
- 11 $\hat{r} = r_{opt}$
- 12 $X_{rotated}(:,\mathcal{I}) \leftarrow 0$
- 13 $X_{rotated} \leftarrow \texttt{ProjectToSphere} (X, \hat{c}, \hat{r}, k)$
- 14 $X_{output} \leftarrow X_{rotated} * R^{-1} + \bar{X}$

end

D Dataset Selection

We select datasets for high- and low-dimensional scenarios, covering both $n \geq d$ and n < d as detailed below. Thanks to the binary search scheme we designed in our SRCA algorithm, SRCA can be parallelized when an even larger n (e.g., n = 100,000) presents. Neither PCA nor non-linear methods we consider below can be generalized to a quite large n in an obvious way.

The tSNE (Van der Maaten and Hinton, 2008) has known problems of not distance-

preserving and creating false clusters in the dimension-reduced dataset (Schubert and Gertz, 2017). The UMAP (McInnes et al., 2018) has known problems of being sensitive to outliers and require the user to have a good understanding of their distance metrics to interpret the dimension-reduced dataset. To highlight the advantage of our method with a geometric loss function, we also choose labeled datasets to study the structure-preserving properties and datasets that require careful normalization.

We use several public datasets for our numerical experiments, but consider only datasets with continuous variables as its features, as we recognized that dimension reduction for datasets with discrete (categorical and integer) or mixed type variables as their attributes is a different problem (Schölkopf et al., 1997, 1998).

Before the analysis of our experiments, we shall briefly introduce our datasets:

• Source

- UCI repository (https://archive.ics.uci.edu/ml): Banknote, Climate, Concrete, Ecoli¹, Leaf, PowerPlant, UserKnowledge.
- Microarray: Alon (Alon et al., 1999).
- GTEx (https://gtexportal.org/home/).

Sample size

We understand that a valid dimension reduction method should have reasonable performance regardless of the size of the underlying datasets. We choose a wide range of datasets with sample sizes varying from 100 to 10,000. In the table below, we show the code for each dataset with its sample size and dimension $(n \times d)$.

n > a	$n \leq a$
Banknote (1372 \times 4), UserKnowledge (403 \times 5),	Kidney Medulla (4×500) ,
Ecoli (336×7) , Concrete (1030×8) ,	Fallopian Tube (9×500) ,
Climate (540×18) , Leaf (340×14) ,	Cervix Endocervix (10×500) ,.
PowerPlant (9568 \times 5),	Alon (62×2000) ,.

Dimensionality

It is of central importance to recognize that the relation between the sample size n and the original dimension d would affect dimension reduction methods. In fact, the sparse PCA (Erichson et al., 2020) were developed to take the sparsity (i.e., n < d) of the dataset into consideration. SRCA has a natural sparsity penalty parameter in the loss function \mathcal{L} we designed. To see the performance of different methods on

¹Three groups among them with sample size smaller than 5 are removed for visual convenience. The five groups left are cytoplasmic proteins (cp), inner membrane proteins without a signal sequence (im), inner brane proteins with an uncleavable signal sequence (imU), other outer membrane proteins (om) and periplasmic proteins (pp).

dense (n > d) and sparse $(n \le d)$ data, we also include both kinds of datasets in the above selection.

Normalization

When the attributes or features of the dataset have high mutual correlation or relationships with one another (e.g., total expenditure cannot exceed total income of an individual), normalization would introduce problems like distortion of correlation and violation of relationships. When the attributes or features of the dataset are uncorrelated or independent, normalization would convert all features to (relatively) the same scale. We include datasets that require normalization and those that do not require normalization.

- Not normalized: Banknote, Ecoli, PowerPlant, UserKnowledge, Climate.
- Normalized: Alon, Concrete, Leaf, GTEx.

Finally, we shall point out that we have not covered any dataset with a high d and large n. Our exploratory experiments found that the performance of existing dimension methods, including modern methods, has suffered from a very high computational cost. It is a separate problem to study how to perform dimension reduction on a large high-dimensional dataset.

Decomposition-based methods like PCA, multi-dimensional scaling (MDS) and truncated singular value decomposition (SVD) become exceedingly slow for a dataset with large n and d. Manifold learning based methods like tSNE, UMAP and IsoMap (Tenenbaum et al., 2000) have some variation in computational time due to their stochastic nature but they are all rather slow. Therefore, we would leave this type of dataset as a separate problem that we do not experiment in the current paper.

E Coranking Performance Comparison for Section 4.3

	SRCA	SPCA	PCA	LLE	tSNE	UMAP
$\overline{\text{CC}}$	0.987	0.925	0.988	0.833	0.640	0.635
AUC	0.869	0.774	0.860	0.598	0.469	0.459
WAUC	0.644	0.582	0.626	0.503	0.694	0.600

Table E.1: Coranking performance scores of Banknote

	SRCA	SPCA	PCA	LLE	tSNE	UMAP
$\overline{\text{CC}}$	0.270	0.270	0.262	0.464	0.215	0.124
AUC	0.152	0.152	0.148	0.225	0.147	0.102
WAUC	0.134	0.132	0.0864	0.105	0.141	0.118

Table E.2: Coranking performance scores of Ecoli

	SRCA	SPCA	PCA	LLE	tSNE	UMAP
$\overline{\text{CC}}$	0.987	0.815	0.987	0.928	0.620	0.847
AUC	0.886	0.605	0.886	0.731	0.446	0.651
WAUC	0.485	0.416	0.485	0.447	0.611	0.528

Table E.3: Coranking performance scores of PowerPlant

	SRCA	SPCA	PCA	LLE	tSNE	UMAP
$\overline{\text{CC}}$	0.219	0.211	0.219	0.183	0.134	0.180
AUC	0.0780	0.0853	0.0785	0.0700	0.0707	0.0635
WAUC	0.0935	0.0952	0.0948	0.0762	0.106	0.100

Table E.4: Coranking performance scores of Leaf

	SRCA	SPCA	PCA	LLE	tSNE	UMAP
$\overline{\text{CC}}$	0.730	0.798	0.693	0.585	0.483	0.592
AUC	0.416	0.456	0.379	0.338	0.231	0.384
WAUC	0.256	0.3233	0.251	0.212	0.214	0.328

Table E.5: Coranking performance scores of Alon.

F Spherical Estimation

The essence of SPCA (Li et al., 2022) can be summarized as a two-step procedure:

- 1. First, we utilize the principal component analysis (PCA) to find a hyper-plane $V \subset \mathbb{R}^{d'+1}$ of retained dimension based on \mathcal{X} and project \mathcal{X} to $\hat{\mathcal{X}}$ in V.
- 2. Second, we perform a circular (or d'-dimensional spherical) regression² with the projected image $\hat{\mathcal{X}}$ onto V.

By selecting the principal components given by PCA, we find a hyper-plane V and determine the dimension of the S. By fitting a circular regression on a d'-dimensional sphere with the projected dataset $\hat{\mathcal{X}}$, we determine the center c and radius r of the spherical support.

²Unfortunately, although methods in circular regression could be extended to spheres of intrinsic dimensions greater than 1, the term "circular regression" instead of "spherical regression" is adopted.

Suppose the assumed sphere $S_V(c,r)$ is $d^2(x,c) = r^2$, whose dimensionality is determined by the PCA estimated linear subspace V. Two typical loss functions for the estimation of c, r are:

$$\mathcal{L}(V, c, r) = \sum_{i=1}^{n} d^2(x_i, S_V(c, r))$$

where d^2 can be chosen as geometric or algebraic loss

geometric loss =
$$\sum_{i=1}^{n} \left(\sqrt{(x_i - c)^T (x_i - c)} - r \right)^2$$
 algebraic loss =
$$\sum_{i=1}^{n} \left((x_i - c)^T (x_i - c) - r^2 \right)^2$$

Following Li et al. (2022), we first assume that V is determined (through PCA) and attempt to estimate the center c and radius r via a two-step gradient descent with both geometric and algebraic loss functions. Through the procedure of taking derivation, we observe and explain why an analytic solution for c and r is impossible in this SPCA setup in the end and how SRCA handles this problem.

F.1 Geometric Loss

Let us calculate the geometric loss first, the algebraic loss is calculated at the end. This function is a quadratic polynomial of radius parameter r > 0, \mathcal{L} has a unique global (conditional) minimum in r if $\hat{r} > 0$. When the c is assumed fixed.

We calculate its gradient

$$\frac{\partial \mathcal{L}(c,r)}{\partial r} = \sum_{i=1}^{n} \frac{\partial}{\partial r} d^{2}(x_{i}, S(c,r))$$

$$= \sum_{i=1}^{n} \frac{\partial}{\partial r} \left(\sqrt{(x_{i} - c)^{T} (x_{i} - c)} - r \right)^{2}$$

$$= \sum_{i=1}^{n} -2 \left(\sqrt{(x_{i} - c)^{T} (x_{i} - c)} - r \right)$$

Setting this equation to zero, we have

$$\hat{r} = \frac{1}{n} \sum_{j=1}^{n} \sqrt{(x_j - c)^T (x_j - c)} \ge 0.$$

Plug this back into the $\mathcal{L}(c,r)$ we have

$$\mathcal{L}(c,\hat{r}) = \sum_{i=1}^{n} d^{2}(x_{i}, S(c, \hat{r}))$$

$$= \sum_{i=1}^{n} \left(\sqrt{(x_{i} - c)^{T} (x_{i} - c)} - \hat{r} \right)^{2}$$

$$= \sum_{i=1}^{n} \left(\sqrt{(x_{i} - c)^{T} (x_{i} - c)} - \frac{1}{n} \sum_{j=1}^{n} \sqrt{(x_{j} - c)^{T} (x_{j} - c)} \right)^{2}$$

Although this cannot be simplified further (due to the fact that it is fourth power in c), we can still attempt to take its gradient

$$\frac{\partial \mathcal{L}(c,\hat{r})}{\partial c} = \sum_{i=1}^{n} \frac{\partial}{\partial c} \left(\sqrt{(x_i - c)^T (x_i - c)} - \frac{1}{n} \sum_{j=1}^{n} \sqrt{(x_j - c)^T (x_j - c)} \right)^2,$$
where $\hat{r} = \frac{1}{n} \sum_{j=1}^{n} \sqrt{(x_j - c)^T (x_j - c)}$

$$= \sum_{i=1}^{n} 2 \left(\sqrt{(x_i - c)^T (x_i - c)} - \hat{r} \right).$$

$$\left(\frac{\partial}{\partial c} \sqrt{(x_i - c)^T (x_i - c)} - \frac{1}{n} \sum_{j=1}^{n} \frac{\partial}{\partial c} \sqrt{(x_j - c)^T (x_j - c)} \right)$$

The equation $\frac{\partial \mathcal{L}(c,\hat{r})}{\partial c} = 0$ would not have an analytic solution in general. However, with an appropriate gradient-based optimization method, for example, Gauss-Newton method with Levenberg-Marquardt correction (Chernov, 2010), the sequence of estimates of c, r can be proven to converge to global minimum under the regularity condition. It is also not hard to observe why the insertion of W into the $\sqrt{(x_i - c)^T W(x_i - c)}$ makes the gradient calculation even more intractable for the geometric loss function.

F.2 Algebraic Loss

However, analytic solutions for a sphere estimation can be derived for algebraic loss. It can also generalize to ellipsoid (i.e., an algebraic loss can be solved analytically for the

ellipsoid $x^T W x = r$)

$$\frac{\partial \mathcal{L}(c,r)}{\partial r} = \sum_{i=1}^{n} \frac{\partial}{\partial r} d^{2}(x_{i}, S(c,r)), \text{ algebraically}$$

$$= \sum_{i=1}^{n} \frac{\partial}{\partial r} \left((x_{i} - c)^{T} (x_{i} - c) - r^{2} \right)^{2}$$

$$= \sum_{i=1}^{n} 2 \left((x_{i} - c)^{T} (x_{i} - c) - r^{2} \right) \cdot (-2r)$$

which is a cubic polynomial. $\frac{\partial \mathcal{L}(c,r)}{\partial r} = 0$ is analytically solvable in r, via Cardano-Viete's formula:

$$0 = \sum_{i=1}^{n} -2\left((x_i - c)^T (x_i - c) - r^2\right) \cdot 2r$$

$$0 = \sum_{i=1}^{n} \left(\left(x_i^T x_i - 2c^T x_i + c^T c\right) - r^2\right) \cdot r$$

$$0 = \sum_{i=1}^{n} \left(\left(x_i^T x_i - 2c^T x_i + c^T c\right) r - r^3\right)$$

$$0 = -n \cdot r^3 + \left[\sum_{i=1}^{n} \left(x_i^T x_i - 2c^T x_i + c^T c\right)\right] \cdot r.$$

Write it into $x^3 + px + q = 0$ form:

$$r^{3} + \left[-\frac{1}{n} \sum_{i=1}^{n} (x_{i}^{T} x_{i} - 2c^{T} x_{i} + c^{T} c) \right] \cdot r + 0 = 0$$
$$p = -\frac{1}{n} \sum_{i=1}^{n} (x_{i}^{T} x_{i} - 2c^{T} x_{i} + c^{T} c), q = 0$$

The determinant $4p^3 + 27q^2 < 0$ obviously, the solution is

$$\hat{r}_k = 2\sqrt{-\frac{p}{3}} \cdot \cos\left[\frac{1}{3}\arccos\left(\frac{3q}{2p}\sqrt{\frac{-3}{p}}\right) - \frac{2\pi k}{3}\right] \text{ for } k = 0, 1, 2.$$

$$= 2\sqrt{\frac{1}{3n}\sum_{i=1}^{n} \left(x_i^T x_i - 2c^T x_i + c^T c\right) \cdot \cos\left[\frac{1}{3} \cdot \frac{\pi}{2} - \frac{2\pi k}{3}\right]}$$

For the gradient with respect to the center c,

$$\frac{\partial \mathcal{L}(c,\hat{r})}{\partial c} = \sum_{i=1}^{n} \frac{\partial}{\partial c} d^{2}(x_{i}, S(c, \hat{r})), \text{ algebraically}$$

$$= \sum_{i=1}^{n} \frac{\partial}{\partial c} \left((x_{i} - c)^{T} (x_{i} - c) - \hat{r}^{2} \right)^{2}$$

$$= \sum_{i=1}^{n} 2 \left(\frac{\partial}{\partial c} \left[(x_{i} - c)^{T} (x_{i} - c) - \frac{1}{n} \sum_{j=1}^{n} (x_{j} - c)^{T} (x_{j} - c) \right] \right)$$

$$= \sum_{i=1}^{n} 2 \left(\frac{\partial}{\partial c} \left[(x_{i}^{T} x_{i} - 2c^{T} x_{i} + c^{T} c) - \frac{1}{n} \sum_{j=1}^{n} (x_{j}^{T} x_{j} - 2c^{T} x_{j} + c^{T} c) \right] \right),$$

and the equation $\frac{\partial \mathcal{L}(c,\hat{r})}{\partial c} = 0$ solves

$$\hat{c} = \frac{1}{2} \left(\sum_{i=1}^{n} (x_i - \frac{1}{n} \sum_{j=1}^{n} x_j)^T (x_i - \frac{1}{n} \sum_{j=1}^{n} x_j) \right)^{-1} \sum_{i=1}^{n} \left(x_i^T x_i - \frac{1}{n} \sum_{j=1}^{n} x_j^T x_j \right) (x_i - \frac{1}{n} \sum_{j=1}^{n} x_j).$$

Therefore, an algebraic loss would provide us a closed form solution to the estimate of both center c and radius r.

F.3 SPCA and SRCA Solution

Following the thought of the simultaneous estimation of c, r and the dimension of the sphere (or equivalently, the linear subspace $\mathbf{V} \in \mathbb{R}^{d \times (d'+1)}$ where S lives in), we can instead consider the following geometric loss in one step

$$\mathcal{L}(V,c,r) = \sum_{i=1}^{n} d^{2}(x_{i}, S_{V}(c,r))$$

$$= \sum_{i=1}^{n} d^{2}(x_{i}, c+V) + \sum_{i=1}^{n} d^{2}(Pr_{V}(x_{i}), S_{V}(c,r))$$

$$= \sum_{i=1}^{n} ||x_{i} - c - VV^{T}(x_{i} - c)||^{2} + \sum_{i=1}^{n} (||Pr_{c+V}(x_{i}) - c|| - r)^{2}$$

$$= \sum_{i=1}^{n} ||x_{i} - c - VV^{T}(x_{i} - c)||^{2} + \sum_{i=1}^{n} (||c + VV^{T}(x_{i} - c) - c|| - r)^{2}$$

$$= \sum_{i=1}^{n} ||x_{i} - c - VV^{T}(x_{i} - c)||^{2} + \sum_{i=1}^{n} (||VV^{T}(x_{i} - c)|| - r)^{2}$$

The second identity comes from the Pythagorean theorem and $Pr_{c+V}(x_i)$ is the linear projection of x_i to the affine subspace c+V.

The first sum corresponds to PCA loss function and the second term is the loss of SRCA if V = I. For the SRCA and the SPCA, we minimize the first sum so V is the top eigenvectors of sample covariance matrices and then plug this V to the second sum, and change the geometric sum to the algebraic loss function, since only the latter loss allows a closed form analytic solution. This minimizer from a two-step procedure obtained by SPCA is not necessarily the same as the true minimizer of the above geometric loss $\mathcal{L}(V, c, r)$. However, these two minimizers coincide when all x_i are from a sphere, otherwise SPCA solution is sub-optimal (Li et al., 2022). We adopt the two-step SPCA algorithm only because we cannot derive a closed form minimizer for $L = \mathcal{L}(V, c, r)$. Moreover, this loss function is difficult to generalize to the ellipsoid situation.

G Related Proofs

G.1 Proof of Theorem 1

For each fixed $||v||_{l_0} = d' + 1$, it suffices to optimize the following sub-problem of (2.5):

$$\min_{c \in \mathbb{R}^d, r \in \mathbb{R}^+} \sum_{i=1}^n \left((x_i - c)^T W(x_i - c) + r^2 - 2r \sqrt{(x_i - c)^T \sqrt{W}^T v^T I v \sqrt{W}} (x_i - c) \right)$$

$$= \min_{c \in \mathbb{R}^d, r \in \mathbb{R}^+} \mathcal{L}_v(c, r; x_1, x_2, \dots, x_n),$$

$$= \min_{c \in \mathbb{R}^d, r \in \mathbb{R}^+} \sum_{i=1}^n \mathcal{L}_v(c, r; x_i),$$
(G.2)

which has gradients with respect to c and r as

$$\frac{\partial \mathcal{L}_{v}}{\partial c} = \sum_{i=1}^{n} \frac{\partial \mathcal{L}_{v}}{\partial c}(c, r; x_{i})$$

$$= \sum_{i=1}^{n} \left(-2(x_{i} - c)^{T} W - 2r \cdot \frac{1}{2} \left[(x_{i} - c)^{T} \sqrt{W}^{T} v^{T} I v \sqrt{W} (x_{i} - c) \right]^{-\frac{1}{2}}$$

$$\left[-2(x_{i} - c)^{T} \sqrt{W}^{T} v^{T} I v \sqrt{W} \right] \right)$$

$$= \sum_{i=1}^{n} -2(x_{i} - c)^{T} \left(W + r \left[(x_{i} - c)^{T} \sqrt{W}^{T} v^{T} I v \sqrt{W} (x_{i} - c) \right]^{-\frac{1}{2}} \left[\sqrt{W}^{T} v^{T} I v \sqrt{W} \right] \right),$$

and,

$$\frac{\partial \mathcal{L}_v}{\partial r} = \sum_{i=1}^n \frac{\partial \mathcal{L}_v}{\partial r}(c, r; x_i) = \sum_{i=1}^n \left(2r - 2\left[\left(x_i - c\right)^T \sqrt{W}^T v^T I v \sqrt{W} \left(x_i - c\right)\right]^{\frac{1}{2}}\right).$$

Therefore, we can assume that the mild assumptions $||x_i - c|| \leq R_1, r \leq R_2$ and $|\lambda_{\max}(W)| \leq R_3$. We can compute the bounds of these gradients, using Cauchy-Schwartz inequality in the first inequality:

$$\|\nabla_{(c,r)}\mathcal{L}_{v}(c,r)\| = \left\|\frac{\partial\mathcal{L}_{v}}{\partial c}(c,r)\right\| + \left\|\frac{\partial\mathcal{L}_{v}}{\partial r}(c,r)\right\|$$

$$\leq 4\sum_{i=1}^{n} (x_{i}-c)^{T}W^{T}W(x_{i}-c)$$

$$\times \sum_{i=1}^{n} \left\|\left(W+r\left[(x_{i}-c)^{T}\sqrt{W}^{T}v^{T}Iv\sqrt{W}(x_{i}-c)\right]^{-\frac{1}{2}}\left[\sqrt{W}^{T}v^{T}Iv\sqrt{W}\right]\right)\right\|^{2}$$

$$+ \sum_{i=1}^{n} \left(2r-2\left[(x_{i}-c)^{T}\sqrt{W}^{T}v^{T}Iv\sqrt{W}(x_{i}-c)\right]^{\frac{1}{2}}\right).$$

$$\leq 4\times 2nR_{3}^{2}\times nR_{1}^{2}\times n\left(R_{3}+R_{2}\frac{\sqrt{R_{3}^{2}}}{\sqrt{R_{1}^{2}}}\right)+n\left(2R_{2}+\sqrt{R_{1}^{2}R_{3}^{2}}\right)$$

$$<\infty$$

For a finite n, we can conclude that \mathcal{L} is Lipschitz with a finite Lipschitz constant as bounded above. Then the gradient descent algorithm would give us a solution to the sub-problem (G.2) with linear convergence from classical results (Boyd et al., 2004). Since for fixed v, each sub-problem converges to the solution, the exhaustive search on v solves the original problem (2.5). In parallel to Boyd et al. (2003), we have proved the Theorem 1.

G.2 Proof of Theorem 3

References we mainly need for our proof below are the formulation in Huber (2004); Huber et al. (1967) and the technical separation lemma in Doob (1953).

We fix the index set \mathcal{I} in the following discussions, and we assume that the parameters to be estimated can be written as a vector $\theta = (c, r) \in \Theta := [-C, C]^d \times [R_0, R] \subset \mathbb{R}^d \times \mathbb{R}^+$, which lies in a (locally) compact space with a countable base $\Theta' = \{[-C, C]^d \cap \mathbb{Q}^d\} \times \{[R_0, R] \cap \mathbb{Q}\}$, the inclusion of $r = R_0$ is needed below for compactness. We denote that estimate for θ based on n samples (by minimization of the \mathcal{L}) by $T_n = T_n(\mathcal{X})$.

The real-valued ρ function, based on the samples $x_1, \dots, x_n \in \mathbb{X} = \mathbb{R}^d$ drawn from the common distribution P defined on the probability space $(\mathbb{X}, \mathcal{A}, \nu)$ with Borel algebra \mathcal{A} and Lebesgue measure ν , is

$$\rho(x;\theta) = \left((x-c)^T W(x-c) + r^2 - 2r \sqrt{(x-c)^T \sqrt{W}^T I_{\mathcal{I}} \sqrt{W} (x-c)} \right)$$

and the $\psi(x;\theta) = \frac{\partial}{\partial \theta} \rho(x;\theta)$ is again differentiable. We show below that the assumptions in Huber et al. (1967) are satisfied, we define our estimator T_n for parameter $\theta = (c,r)$ such that

$$\frac{1}{n} \sum_{i=1}^{n} \rho(x_i; T_n) - \inf_{\theta \in \Theta} \frac{1}{n} \sum_{i=1}^{n} \rho(x_i; \theta) \to 0, \text{a.s. } P$$
 when $n \to \infty$

corresponding to case A in Huber et al. (1967). Since ρ is differentiable in both x, θ , this minimizer could also be expressed in form of T_n satisfying

$$\frac{1}{\sqrt{n}} \sum_{i=1}^{n} \psi(x_i; T_n) \to 0, \text{a.s. } P$$
 when $n \to \infty$

• (A-1) For $\Theta = \mathbb{R}^d \times \mathbb{R}^+$, there exists a countable basis $\Theta' = \{[-C, C]^d \cap \mathbb{Q}^d\} \times \{[R_0, R] \cap \mathbb{Q}\}$ such that for every open set $U \subset \Theta$ and every closed interval $A \subset \mathbb{R}$, two sets

$$\{x \mid \rho(x;\theta) \in A \in \mathcal{A}, \forall \theta \in U\}$$
$$\{x \mid \rho(x;\theta) \in A \in \mathcal{A}, \forall \theta \in U \cap \Theta'\}$$

would only differ on the set of zero probability measure P. Since the measure P is fixed, by Lemma 2.1 on page 56 of Doob (1953), for each $\theta \in \Theta$ we can find $\theta' \in \Theta'$ such that

$$P\left\{\omega \in \mathbb{X} \mid \rho(x(\omega); \theta) \neq \rho(x(\omega); \theta'), x(\omega) \sim P\right\} = 0.$$

Therefore, denote the map $\tau_P:\theta\mapsto\theta'$ we can redefine our ρ by $\tilde{\rho}:=\rho\circ\tau_P$ so that it only differs from ρ on a zero measure set of the fixed P. Note that the mapping τ_P depends on the measure P and we assume P is fixed throughout our discussion. This ensures the measurability of $\inf_{\theta'\in U}\tilde{\rho}(x;\theta')$ and the measurability of its limit when an (open) neighbor hood U of θ shrinks to one-point set $\{\theta\}$. For ease of notation, we still use ρ below as assume (A-1) holds.

• (A-2) The function ρ is continuous and differentiable, therefore clearly lower semicontinuous in $\theta = (c, r)$. And this ensures that $\inf_{\theta' \in U} \rho(x; \theta') \to \rho(x; \theta)$. • (A-3) There exists a measurable function a(x) such that

$$\mathbb{E}_{P} (\rho(x; \theta) - a(x))^{-} < \infty$$

$$\mathbb{E}_{P} (\rho(x; \theta) - a(x))^{+} < \infty$$

and hence $\gamma(\theta) = \mathbb{E}(\rho(x,\theta) - a(x))$ is well-defined for all $\theta \in \Theta$. For our purpose, we choose $\theta_1 = (c_1, r_1)$ for some $||c_1|| < \infty$ and $r_1 < \infty$. We define a function on \mathbb{X}

$$a(x) = a_{\theta_1}(x) = \left((x - c_1)^T W(x - c_1) + r_1^2 - 2 \cdot r_1 \sqrt{(x - c_1)^T \sqrt{W}^T} I_{\mathcal{I}} \sqrt{W} (x - c_1) \right)$$

$$\rho(x; \theta) - a(x) = \left((x - c)^T W(x - c) - (x - c_1)^T W(x - c_1) \right) + \left(r^2 - r_1^2 \right)$$

$$- 2r \sqrt{(x - c)^T \sqrt{W}^T} I_{\mathcal{I}} \sqrt{W} (x - c)$$

$$+ 2r_1 \sqrt{(x - c_1)^T \sqrt{W}^T} I_{\mathcal{I}} \sqrt{W} (x - c_1)$$

$$\leq |\lambda_{\max}(W)| \left(||x - c||^2 - ||x - c_1||^2 \right) + \left(r^2 - r_1^2 \right)$$

$$+ 4 \max(r, r_1) \cdot \max(||c||, ||c_1||) \cdot |\lambda_{\max}(W)| \cdot ||x||$$

If we take \mathbb{E}_P on both sides of inequality above and with the assumption that $|\lambda_{\max}(W)| < R_3$, then the mild assumption that P has finite second moments (hence finite first moment) ensures the finiteness. It is not hard to see that the choice of θ_1 is not essential in verifying this assumption. For simplicity, we assume $\theta_1 = (c_1, r_1) = (0, 1)$ hereafter.

$$a(x) = \left(|\lambda_{\max}(W)| ||x||^2 + 1 - 2\sqrt{x^T \sqrt{W}^T I_{\mathcal{I}} \sqrt{W} x} \right)$$

• (A-4) There is a $\theta_0 \in \Theta$ such that $\gamma(\theta) > \gamma(\theta_0)$ for all $\theta \neq \theta_0$. To see this, we use the Fubini theorem to take differentiation inside the \mathbb{E}_P (note that this is taken with respect to x) to conclude unique minima of $\gamma(\theta)$ (notice that we assume \mathcal{I} fixed and therefore the index vector v is a fixed constant vector)

$$\gamma(\theta) = \mathbb{E}_{P}\rho(x;\theta) - a(x)
= \mathbb{E}_{P}\left((x-c)^{T}W(x-c) + r^{2} - 2r\sqrt{(x-c)^{T}\sqrt{W}^{T}I_{\mathcal{I}}\sqrt{W}}(x-c)\right) - a(x)
\frac{\partial}{\partial \theta}\gamma(\theta) = \mathbb{E}_{P}\left(\frac{\partial}{\partial c}\rho(x;\theta)\right)
= \begin{pmatrix} -\mathbb{E}_{P}2(x-c)^{T}\left(W + r\left[(x-c)^{T}\sqrt{W}^{T}v^{T}I_{p}v\sqrt{W}(x-c)\right]^{-\frac{1}{2}}\left[\sqrt{W}^{T}v^{T}I_{p}v\sqrt{W}\right]\right) \\
\mathbb{E}_{P}2r - 2\left[(x-c)^{T}\sqrt{W}^{T}v^{T}I_{p}v\sqrt{W}(x-c)\right]^{\frac{1}{2}} \\
= 0$$

By letting $\frac{\partial}{\partial \theta} \gamma(\theta) = 0$ and for $x \sim P$, we derive from the second equation that

$$r_0(c) = \mathbb{E}_P \left[(x - c)^T \sqrt{W}^T v^T I_p v \sqrt{W} (x - c) \right]^{\frac{1}{2}} \in [0, \min(R, 2C\sqrt{|\lambda_{\max}(W)|})],$$

and from the first equation

$$\mathbb{E}_{P} 2 (x - c)^{T} \left(W + r_{0}(c) \left[(x - c)^{T} \sqrt{W}^{T} v^{T} I_{p} v \sqrt{W} (x - c) \right]^{-\frac{1}{2}} \left[\sqrt{W}^{T} v^{T} I_{p} v \sqrt{W} \right] \right) = 0$$

Consider the following function

$$F(c) := \mathbb{E}_P 2 (x - c)^T \left(W + r_0(c) \left[(x - c)^T \sqrt{W}^T v^T I_p v \sqrt{W} (x - c) \right]^{-\frac{1}{2}} \right]$$
$$\left[\sqrt{W}^T v^T I_p v \sqrt{W} \right]$$
(G.3)

as a function of c and the above equation becomes F(c) = 0. Taking a sandwiching-style argument, we first note that the second term in the second bracket is always non-negative, then we construct uniform bounding functions:

$$F_{1}(c) := \mathbb{E}_{P} 2 (x - c)^{T} W$$

$$\approx \mathbb{E}_{P} (x - c)^{T} W,$$

$$F_{2}(c) := \mathbb{E}_{P} 2 (x - c)^{T} \left(W + \min(R, 2C\sqrt{|\lambda_{\max}(W)|}) + |\lambda_{\max}(W)| \left[(x - c)^{T} \sqrt{W}^{T} v^{T} I_{p} v \sqrt{W} (x - c) \right]^{-\frac{1}{2}} \right) W$$

$$\approx \mathbb{E}_{P} (x - c)^{T} \left(1 + \frac{K(R, C, v, |\lambda_{\max}(W)|)}{\|x - c\|_{2}} \right) W,$$

(where $K(R,C,v,|\lambda_{\max}(W)|)$ is a non-negative constant) such that the following bound $F_1(c) \leq F(c) \leq F_2(c)$ holds (for each component of the vector-valued F_1,F_2) uniformly in c. However, it is clear that there exists $c_1^+, c_2^- \in [-C,C]^d \subset \mathbb{R}^d$

$$F(c_1^+) \ge F_1(c_1^+) > 0,$$

 $F(c_2^-) \le F_2(c_2^-) < 0.$

Note that F is continuous in c (we can take derivative under \mathbb{E}_P since P is assumed to possess finite second moment) and $[-C, C]^d$ is connected, we apply the multivariate intermediate value theorem to assert the existence of \mathbf{a} solution c_0 for F(c) = 0. Therefore, we can keep this solution c_0 , which we know its existence but do not know its expression. Back substitution of this solution of c_0 into the expression of r_0 yields

$$r_0 = \mathbb{E}_P \left[(x - c_0)^T \sqrt{W}^T v^T I_p v \sqrt{W} (x - c_0) \right]^{\frac{1}{2}},$$

where $\theta_0 = (c_0, r_0)$ is well-defined for P with finite second moment. This verifies the assumption (A-4).

• (A-5) With the notations in (A-3), since $\Theta := [-C, C]^d \times [R_0, R] \subset \mathbb{R}^d \times \mathbb{R}^+$ is a compact space, it suffices to verify only (i) of (A-5). There is a continuous function $b(\theta) > 0$ such that

$$b(\theta) = \left(c^T W c + r^2 - 2r \sqrt{c^T \sqrt{W}^T} I_{\mathcal{I}} \sqrt{W} c\right) + 1 \in [1, 1 + C^2 |\lambda_{\max}(W)| + R^2]$$

For a fixed $x \in \mathbb{X}$, the function $g_x(\theta) = 2r\sqrt{(x-c)^T\sqrt{W}^TI_{\mathcal{I}}\sqrt{W}(x-c)}$ has gradient

$$\frac{\partial}{\partial \theta} g_x(c,r) = \begin{pmatrix} \frac{\partial}{\partial c} g_x(c,r) \\ \frac{\partial}{\partial r} g_x(c,r) \end{pmatrix}$$

$$= \begin{pmatrix} r \left[(x-c)^T \sqrt{W}^T I_{\mathcal{I}} \sqrt{W} (x-c) \right]^{-\frac{1}{2}} \cdot 2 (x-c)^T \sqrt{W}^T I_{\mathcal{I}} \sqrt{W} \\ 2\sqrt{(x-c)^T \sqrt{W}^T} I_{\mathcal{I}} \sqrt{W} (x-c) \end{pmatrix}$$

which is bounded from above in matrix norm by $2R\sqrt{|\lambda_{\max}(W)|} \cdot 4RC\sqrt{|\lambda_{\max}(W)|} \le 16\max(R^2, 1) \cdot C|\lambda_{\max}(W)| =: L_g < \infty$. Therefore, the function $g_x(c, r)$ is a L_g -

Lipschitz function. We have

$$\inf_{\theta \in \Theta} \frac{\rho(x;\theta) - a(x)}{b(\theta)} = \inf_{\theta \in \Theta} \left\{ \left((x-c)^T W(x-c) - x^T W x \right) + \left(r^2 - 1 \right) \right.$$

$$\left. - 2r \sqrt{(x-c)^T \sqrt{W}^T I_{\mathcal{I}} \sqrt{W}} \left(x - c \right) + 2\sqrt{x^T \sqrt{W}^T I_{\mathcal{I}} \sqrt{W} x} \right\}$$

$$\left(c^T W c + r^2 - 2r \sqrt{c^T \sqrt{W}^T I_{\mathcal{I}} \sqrt{W}} c + 1 \right)^{-1}$$

$$\geq \inf_{\theta = (c,r) \in \Theta} \left\{ \left((x-c)^T W(x-c) - x^T W x \right) + \left(r^2 - 1 \right) \right.$$

$$\left. - 2r \sqrt{(x-c)^T \sqrt{W}^T I_{\mathcal{I}} \sqrt{W}} \left(x - c \right) + 2\sqrt{x^T \sqrt{W}^T I_{\mathcal{I}} \sqrt{W}} x \right\}$$

$$\left(1 + C^2 |\lambda_{\max}(W)| + R^2 \right)^{-1} =: h(x)$$

and $\frac{\rho(x,\theta)-a(x)}{b(\theta)} \ge h(x)$ by the infimum in the definition while h(x) is integrable with respect to P due to the fact that $g_x(c,r)$ is Lipschitz.

Now we verify all assumptions (A-1) to (A-5) in Huber et al. (1967), Theorem 1 in the same paper ensures that Theorem A holds. The mild assumptions that θ lies in a compact subspace of $\mathbb{R}^d \times \mathbb{R}^+$ can be relaxed by verifying a more stringent set of conditions (A-5) as pointed out by Huber et al. (1967). Since we actually verify assuming that the index set \mathcal{I} is fixed, we need to point out that in the l_0 optimization for each fixed \mathcal{I} the consistency result holds. But for the l_1 relaxed problem, we cannot guarantee consistency even with stronger assumptions, only algorithmic convergence is guaranteed.

G.3 Proof of Theorem 4

Now we take the second view that the estimator sequence T_n for parameter $\theta = (c, r)$ and assume a fixed index set \mathcal{I} such that

$$\frac{1}{n} \sum_{i=1}^{n} \psi(x_i; T_n) \to 0, \text{ a.s. } P$$
$$n \to \infty,$$

• (N-1) For each fixed $\theta \in \Theta$, $\psi(x;\theta)$ is \mathcal{A} -measurable and separable. Like the construction in (A-1), we can modify the ψ into a separable version $\tilde{\psi}$ if necessary and verify this assumption. Then following functions are well-defined (with finite second

moment assumption on P and the Fubini theorem)

$$\lambda(\theta) = \lambda(c, r) := \mathbb{E}_{P} \psi(x; \theta)$$

$$= \mathbb{E}_{P} \frac{\partial}{\partial \theta} \rho(x; \theta)$$

$$= \frac{\partial}{\partial \theta} \mathbb{E}_{P} \rho(x; \theta)$$

$$u(x, \theta, D) = \sup_{\|\tau - \theta\| \le D} |\psi(x; \tau) - \psi(x; \theta)|.$$

- (N-2) The same θ_0 as computed above would satisfy $\lambda(\theta_0) = 0$.
- (N-3) There are strictly positive numbers $\alpha, \beta, \gamma, \eta$ such that
 - (i) $|\lambda(\theta)| \ge \alpha |\theta \theta_0|$ for some $\alpha > 0$ and $|\theta \theta_0| \le \eta$ is clear since

$$\lambda(\theta) = \frac{\partial}{\partial \theta} \mathbb{E}_P \left((x - c)^T W (x - c) + r^2 - 2r \sqrt{(x - c)^T \sqrt{W}^T} I_{\mathcal{I}} \sqrt{W} (x - c) \right)$$

is quadratic in both c and r, and it is bounded from below by linear part due to Taylor expansion at θ_0 .

- (ii) $\mathbb{E}_P u(x, \theta, D) = \mathbb{E}_P \sup_{\|\tau - \theta\| \le D} |\psi(x; \tau) - \psi(x; \theta)| \le \mathbb{E}_P \beta \|\tau - \theta\|$ since $\frac{\partial}{\partial r} \psi(x; \theta) = 2$ and

$$\frac{\partial}{\partial c}\psi(x;\theta) = \mathbb{E}_{P}2c^{T}\left(W + r\left[(x-c)^{T}\sqrt{W}^{T}v^{T}Iv\sqrt{W}(x-c)\right]^{-\frac{1}{2}}\left[\sqrt{W}^{T}v^{T}Iv\sqrt{W}\right]\right)$$

$$-\mathbb{E}_{P}2(x-c)^{T}\left(-\frac{1}{2}r\left[(x-c)^{T}\sqrt{W}^{T}v^{T}Iv\sqrt{W}(x-c)\right]^{-\frac{3}{2}}\right]$$

$$\cdot 2(x-c)^{T}\sqrt{W}^{T}v^{T}Iv\sqrt{W}\cdot\left[\sqrt{W}^{T}v^{T}Iv\sqrt{W}\right]\right)$$

$$\leq 2CR(1 + (4C^{2}|\lambda_{\max}(W)|^{-\frac{1}{2}})|\lambda_{\max}(W)|$$

$$+4C\left(R\cdot(4C^{2}|\lambda_{\max}(W)|^{-\frac{3}{2}}\cdot2C|\lambda_{\max}(W)|^{2}\right)$$

$$\leq 16CR(4C^{2}|\lambda_{\max}(W)|^{-\frac{1}{2}}\max(|\lambda_{\max}(W)|,1)^{4} + |\lambda_{\max}(W)| < \infty.$$

And $\psi(x;\theta)$ is Lipschitz with coefficient

$$\beta := 32CR(4C^2|\lambda_{\max}(W)|^{-\frac{1}{2}}\max(|\lambda_{\max}(W)|, 1)^4 + |\lambda_{\max}(W)|.$$

- (iii)
$$\mathbb{E}_{P}u(x,\theta,D)^{2} = \mathbb{E}_{P}\left(\sup_{\|\tau-\theta\|\leq D}|\psi(x;\tau)-\psi(x;\theta)|\right)^{2} \leq \max\left\{\mathbb{E}_{P}\left(\beta\|\tau-\theta\|\right)^{2},\left(\mathbb{E}_{P}\beta\|\tau-\theta\|\right)^{2}\right\}$$
 and for $\gamma=\beta$ we can replace $\|\tau-\theta\|\leq 1$

 $\eta - D$ with $\eta - D$.

• (N-4) $\mathbb{E}_P\left[|\psi(x;\theta_0)|^2\right] < \infty$ is clear from the analytic expression of $\psi(x;\theta)$, which involves at most quadratic entries in x, and the fact that we assume P has finite second moments.

Assumptions (N-1) through (N-4) allow us to apply Theorem 3 and its corollary in Huber et al. (1967) and claim Theorem B. The asymptotic normality result allows us to claim a Wald-type hypothesis testing for the estimated center and radius for the sphere for a fixed index set \mathcal{I} . that aspect in the current paper but point out that this is one of the few non-bootstrap hypothesis testing methods in manifold learning literature.

H Mean Square Errors for Out-of-sample Data

This appendix provides the out-of-sample mean square errors of PCA, SPCA and SRCA on the same datasets in Table 4.1. We provide this to show that performance evaluation measures are not really affected by the choice of testing samples.

Dataset	$\mathrm{Method}/d' =$	1	2	3	4
	PCA	15.6094	6.2737	1.9278	
Banknote	SPCA	15.0516	7.3182	1.5511	
	SRCA	13.2273	5.4120	1.1257	
Power	PCA	227.6291	56.0524	23.4302	3.0244
Plant	SPCA	151.7555	102.3262	44.3802	41.0081
	SRCA	151.3426	52.9769	20.0871	4.0775
User	PCA	0.1952	0.1281	0.0749	0.0306
Knowledge	SPCA	0.1478	0.0898	0.0465	0.0145
	SRCA	0.1479	0.0904	0.0462	0.0144
	PCA	0.0761	0.0334	0.0219	0.0057
Ecoli	SPCA	0.0462	0.0351	0.0187	0.0122
	SRCA	0.0758	0.0337	0.0168	0.0058
	PCA	6.8783	4.8345	3.5462	2.5046
Concrete	SPCA	5.5565	4.2051	3.1664	2.0173
	SRCA	5.5573	4.2173	3.1842	2.0389
	PCA	0.0245	0.0126	0.0062	0.0040
Leaf	SPCA	0.0163	0.0100	0.0073	0.0047
	SRCA	0.0164	0.0101	0.0062	0.0037
	PCA	1.4486	1.3846	1.3167	1.2447
Climate	SPCA	1.4265	1.3637	1.2921	1.2224
	SRCA	1.3863	1.3081	1.2278	1.1525

 ${\bf Table~H.1:}~ {\bf Out\text{-}of\text{-}sample~mean~square~error~(MSE)~table~for~different~experiments}.$